https://doi.org/10.5194/hess-2021-355
Preprint. Discussion started: 8 July 2021

Hydrology and Earth System Sciences Discussions

Tandem use of transit time distribution and fraction of young water reveals the dynamic flow paths supporting streamflow at a mountain headwater catchment

Ravindra Dwivedi[1], Christopher Eastoe[2], John F. Knowles[3], Jennifer McIntosh[1], Thomas Meixner[1], Ty P.A. Ferre[1], Rebecca Minor[3,4], Greg Barron-Gafford[3,4], Nathan Abramson[1], Michael Stanley[5], and Jon Chorover[6]

[1]Department of Hydrology and Atmospheric Sciences, The University of Arizona, Tucson, AZ, U.S.A.

[2]Department of Geosciences (retired), The University of Arizona, Tucson, AZ, U.S.A.

[3]School of Geography, Development & Environment, The University of Arizona, Tucson, AZ, U.S.A.

[4]Biosphere 2, The University of Arizona, Tucson, AZ, U.S.A.

[5]Mt. Lemmon Water District, Tucson, AZ, U.S.A.

[6]Department of Environmental Science, The University of Arizona, Tucson, AZ, U.S.A.

Correspondence to: Ravindra Dwivedi (ravindradwivedi@email.arizona.edu)

https://doi.org/10.5194/hess-2021-355
Preprint. Discussion started: 8 July 2021

Hydrology and Earth System Sciences Discussions

Abstract. Current understanding of the dynamic flow paths and subsurface water storages that support streamflow in mountain catchments is inhibited by the lack of long-term hydrologic data and the frequent use of single age tracers that are not applicable to older groundwater reservoirs. To address this, the current study used both multiple metrics and tracers to characterize the transient nature of flow paths with respect to change in catchment storage at Marshall Gulch, a sub-humid headwater catchment in the Santa Catalina Mountains, Arizona, USA. The fraction of streamflow that was untraceable using stable water isotope tracers was also estimated. A Gamma-type transit time distribution (TTD) was appropriate for deep groundwater analysis, but there were errors in the TTD shape parameters arising from the short record length of ^{3}H in deep groundwater and stream water, and inconsistent seasonal cyclicity of the precipitation ^{3}H time series data. Overall, the mean transit time calculated from ^{3}H data was more than two decades greater than the mean transit time based on δ^{18}O at the same site. The fraction of young water (F_{yw}) in shallow groundwater was estimated from δ^{18}O time series data using weighted wavelet transform (WWT), iteratively re-weighted least squares (IRLS), and TTD-based methods. Estimates of F_{yw} depended on sampling frequency, the method of estimation, bedrock geology, hydroclimate, and factors affecting streamflow generation processes. The coupled use of F_{yw} and discharge sensitivity indicated highly dynamic flow paths that reorganized with changes in shallow catchment storage. The utility of ^{3}H to determining F_{yw} in deeper groundwater was limited by data quality. Given that F_{yw}, discharge sensitivity, and mean transit time all yield unique information, this work demonstrates how co-application of multiple methods can yield a more complete understanding of the transient flow paths and observable storage volumes that contribute to streamflow in mountain headwater catchments.

https://doi.org/10.5194/hess-2021-355
Preprint. Discussion started: 8 July 2021

1 Introduction

Mountain headwater catchments are critical sources of water to downstream valley-fill aquifers (Viviroli et al., 2007;Viviroli et al., 2003;Kohler and Marselli, 2009;Carroll et al., 2019;Milly and Dunne, 2020;Harpold et al., 2012;Eppolito and Fonseca, 2021;Bryan, 2021). However, the conditions under which shallow and deep subsurface water storages and transient flow paths support streamflow in complex mountain terrain are still incompletely understood (McDonnell et al., 2018;McDonnell, 2017). Sustainable Development Goal (SDG) #15 of the 2030 Agenda for Sustainable Development (United Nations, 2015) specifically lists this shortcoming as a major hurdle to attaining sustainable development (United Nations, 2021;Creed and Noordwijk, 2018). Therefore, additional research is needed to thoroughly characterize dynamic relationships between storage, flow paths, and streamflow in the mountains.

Dual tracer approaches using stable water isotopes and tritium (^3H) are recommended to determine the contribution of deep groundwater to streamflow in mountain sites characterized by fractured bedrock aquifers (Stewart et al., 2010;Stewart et al., 2012). This recommendation originates from previous work that shows how mean transit time (mTT) estimates based on stable water isotopes alone may be underestimated because the tails of the transit time distributions (TTDs) that correspond to longer transit times can become truncated (Stewart et al., 2010;Stewart et al., 2012;Frisbee et al., 2013;DeWalle et al., 1997), and additionally takes into consideration that certain model performance criteria (e.g., Nash-Sutcliffe Efficiency) are insensitive to longer transit times (Seeger and Weiler (2014). Underestimated transit times can have cascading impacts on subsurface weathering rates, leading to incorrect understanding of stream water chemistry (Frisbee et al., 2013;Clow et al., 2018). As a result, the current

https://doi.org/10.5194/hess-2021-355
Preprint. Discussion started: 8 July 2021

study leverages the use of ^{3}H as a tracer with longer-period variations as a means to more completely characterize deeper flow paths that contribute to streamflow.

Using a virtual or synthetic experimental model setup and stable water isotope data, Kirchner (2016b, 2016a) identified significant aggregation errors in mTT estimates for heterogeneous catchments. As an alternative, Kirchner (2016b, 2016a) proposed the fraction of young water metric (F_{yw}), i.e., the fraction of water that has resided in a catchment for less than a threshold period of time, that is largely insensitive to spatial and temporal aggregation errors when evaluated for annual tracer cycles in inflow and outflow. Using a similar virtual experimental model setup but with ^{3}H as a tracer, Stewart et al. (2017) also noted spatial aggregation errors in mTT but not F_{yw}. Together, these results suggest that catchment storage estimates based on F_{yw} should be robust. Importantly, these and other F_{yw}-based studies (Jasechko et al. (2016); von Freyberg et al. (2018); Gallart et al. (2020a); Clow et al. (2018); Gallart et al. (2020a); Jacobs et al. (2018); Stockinger et al. (2016); Jasechko et al. (2017); Table S6; Table 2) considered annual or seasonal cycles in stable water isotope data or only one period when using only tritium (Stewart et al., 2017) or both tracers (Rodriguez et al., 2021); the authors know of no previous studies that have considered both ^{3}H and δ^{18}O tracers and multiple periods.

When F_{yw} is related to the discharge flux, it contributes to a more thorough understanding of groundwater flow path dynamics and thus water quantity and quality in headwater catchments. Accordingly, the resulting discharge sensitivity of F_{yw} can be considered the "diagnostic finger print" for streamflow generation processes. In this way, von Freyberg et al. (2018) distinguished between sites in terms of dominant flowpaths and flowpath changes during large and small storms, and suggested evaluation of their framework in different climatic and geological settings. Gallart et al. (2020b) applied

https://doi.org/10.5194/hess-2021-355
Preprint. Discussion started: 8 July 2021

Hydrology and Earth System Sciences Discussions

an alternative formulation for discharge sensitivity to a sub-humid Mediterranean field site, again concluding that flow paths responded dynamically to precipitation flux. Similar conclusions resulted from studies of alluvial and lower-elevation mountain-block aquifers in Arizona, USA (Eastoe and Wright, 2019;Eastoe and Towne, 2018) where recharge only occurred during the wettest ~30% of months. In this study, F_{yw} is considered along with discharge sensitivity to better understand the degree to which catchment storage and flow paths are interrelated.

The current study addresses the following research questions at a high-elevation, sub-humid mountain site: (i) what is the appropriate TTD type and mTT for the deep groundwater system that supports streamflow? (ii) What are the F_{yw} and resulting F_{yw}-based catchment storage estimates calculated from age tracers applicable to younger and older groundwater and stable water isotope and ^{3}H time series data, respectively? (iii) What is the discharge sensitivity of F_{yw} as determined by stable water isotope tracers? Following a description of the field site and data, we describe theoretical models and estimation methods for ^{3}H-based TTD and mTT estimation and F_{yw} (using both stable water isotopes and ^{3}H) and its discharge sensitivity (stable water isotopes only). We discuss potential reasons for bias in the F_{yw} literature toward both stable isotope tracers and annual cyclic variations and broaden the F_{yw} approach by using both stable water isotope and ^{3}H tracers simultaneously. The present study complements Dwivedi et al. (2021) who estimated TTD and mTT for shallow groundwater storages at the same study site using gamma distributions fitted to stable water isotope time series data in precipitation and streamflow.

https://doi.org/10.5194/hess-2021-355
Preprint. Discussion started: 8 July 2021

Hydrology and Earth System Sciences Discussions

2 Study site and data

2.1 Study site

The study site was the Marshall Gulch catchment (MGC), a 1.55 km^2 headwater catchment located within the Santa Catalina Mountains ~26 km northeast of Tucson in southeast Arizona, USA (Figure 1). The elevation at MGC ranges from 2285 to 2632 m above sea level (asl) with a mean of 2428 m asl and a mean topographic slope of 22^o (or ~40%). Bedrock at the field site is mostly granite at upper elevations and micaceous schist at lower elevations (Dickinson et al., 2002). The prevailing soil type is sandy loam (Holleran, 2013b) with soil depth varying from 0 m to 1.5 m (Pelletier and Rasmussen, 2009). Soils overlying micaceous schist are generally deeper and have a higher clay content than soils overlying granite (Heidbüchel et al., 2013;Holleran, 2013a). Based on a 30-year (1981-2010) record, the long-term average annual precipitation at MGC is 920 mm (PRISM Climate Group, 2018). The catchment received an average of 654 mm (±158 mm) of precipitation per year between water years (WY) 2008 through 2017; the mean annual streamflow for the same period was 247 mm (±138 mm). WY *n* is defined here as the period from July 1 of year *n-1* through June 30 of year *n*. Instrumentation relevant to this study within and around the field site is shown in Figure 1.

2.2 Data

2.2.1 Hydrologic fluxes

The MGC-scale daily precipitation (P) and streamflow (Q) data were calculated between WY 2008 and 2017 (Figure 2A; Dwivedi et al. (2019a);Dwivedi et al. (2020)). Precipitation was observed at 15-minute

https://doi.org/10.5194/hess-2021-355
Preprint. Discussion started: 8 July 2021

Hydrology and Earth System Sciences Discussions

intervals at eight measurement sites equipped with tipping bucket precipitation gages at seven locations and a heated precipitation gage at the remaining site (Figure 1). From the precipitation time series, Thiessen polygon-derived weights were used to estimate daily catchment-scale mean precipitation (Dwivedi et al., 2019a). Streamflow was measured at 30-minute intervals at the MG-Weir site (Figure 1) using a pressure transducer (U20-001-01; Onset) with maximum error of 0.62 kPa and accuracy of 0.02 kPa and a previously derived stage-discharge relationship (Heidbüchel et al., 2012).

2.2.2 Stable water isotope data in precipitation and streamflow

2.2.2.1 Precipitation

The precipitation bulk samples at MGC were collected using bulk samplers at the Schist, Fern Valley, and Granite station and using ISCO autosamplers at the MG-Weir and Mt. Lemmon stations (Figure 1). At the Fern Valley, Granite, and Schist stations, two collectors were installed at each station and samples were collected every 5 to 7 days (Heidbüchel et al. (2012); Lyon et al. (2009). At the Mt. Lemmon and MG-Weir stations, daily bulk precipitation samples were collected. At the Mt. Lemmon station, sampling mainly focused on summer monsoons (Heidbüchel et al., 2012), whereas continuous samples were collected beginning in December 2009 at the MG-Weir station. At all stations, the data density decreased after 2012 (see Figure 2B). The catchment-scale time series of $\delta^{18}O$ in precipitation was calculated as the unweighted mean of results from all stations and was characterized by irregular time intervals between WY 2008 through WY 2012. (Heidbüchel et al. (2012); Dwivedi et al. (2021).

https://doi.org/10.5194/hess-2021-355
Preprint. Discussion started: 8 July 2021

Hydrology and Earth System Sciences Discussions

2.2.2.2 Streamflow

Stream water samples were collected using an autosampler installed at the MG-Weir site prior to 2012 and by grab sampling after 2012 (Figure 2B). While the stream water autosampler collected daily samples, sub-daily samples were also collected on the rising and falling limbs of the hydrograph during large runoff events (Heidbüchel et al., 2012). In the current study, sub-daily samples are volume-weighted to daily resolution (Dwivedi et al., 2021) .

2.2.3 Tritium in precipitation, streamflow and deep groundwater

We calculated the amount-weighted time series of ^3H in Tucson precipitation since 1992 following (i) Eastoe et al. (2004), (ii) The Environmental Isotope Laboratory, The University of Arizona, (access date: September 26, 2017); and (iii) Dr. C. Eastoe, unpublished data. At low levels of ^3H concentration in precipitation, the data have a 1σ precision of ± 0.5 TU (tritium units) or less. Annual concentration cycles in the ^3H data are best captured by the post-2001 period, which corresponds to semi-annual aggregates representing all precipitation events; between 1992 and 2001, the data represent large precipitation events only. Prior to 1992, mean annual ^3H concentrations in Tucson precipitation were modeled from Doney et al. (1992) or interpolated (hollow squares) between observed or modeled values to obtain amount-weighted precipitation ^3H concentrations at the half-yearly time scale (Figure S1A). All data were corrected for the elevation difference between the Tucson (747 m asl) and MGC (mean elevation 2428 m asl) by using the ^3H concentrations in three simultaneous precipitation samples (Figure S1B) from Tucson and the Palisades Ranger Station, Santa Catalina Mountains. Input ^3H time series data are shown in Figures 3 and S1C. The ^3H time series data for deep groundwater was composed of observations in streamflow (baseflow conditions; n = 9) and groundwater from fractured bedrock (n = 5; Table S1; top

https://doi.org/10.5194/hess-2021-355
Preprint. Discussion started: 8 July 2021

Hydrology and Earth System Sciences Discussions

right inset). Additionally, the five discharge measurements from Pigeon Spring (Figure 1) were considered representative of deep groundwater (Dwivedi et al., 2019b). Data are grouped into half-yearly brackets using the following criteria: (i) sampling months 6 to 10 of year n, and (ii) sampling months 11 of year n-1 to 5 of year n. For groups with three or more measurements, the data are expressed as a mean $\pm$ 1σ (Fig. 3 inset).

3 Method description and previous results

3.1 Multi-tracer based TTD and mTT estimation methods

3.1.1 Stable water isotope-based TTD and mTT estimates

Dwivedi et al. (2021) proposed an improved practical approach for estimating the TTD of stream water using long-term measurements of hydrologic fluxes and $\delta^{18}O$ in precipitation and streamflow. Evaluating multiple TTD types and using the weighted wavelet spectral analysis method of Kirchner and Neal (2013), they determined that a combined Piston Flow and Gamma TTD was applicable for periods of up to one month, and that a Gamma TTD was applicable thereafter. The resulting Gamma TTD shape parameter (α) was 0.42±0.001 (dimensionless) and the mTT was 0.82±0.03 years.

3.1.2 Tritium-based TTD and mTT estimation

Previous work determined that deep groundwater at MGC was recharged at a time scale of 0.5 years or less on the basis of end-member mixing analysis (Ajami et al. (2011);Dwivedi et al. (2019b). Here, we use time series ^{3}H data to expand on these results. Given that these data are only available at seasonal

https://doi.org/10.5194/hess-2021-355
Preprint. Discussion started: 8 July 2021

resolution (Section 2.2.3; Figure 3), the Stewart et al. (2016) method, i.e., Equation (1) below, was used to estimate the mean transit time and best fitting TTDs:

$$C_Q(t) = \int_0^\infty C_{Recharge}(t-\tau)\, e^{-\frac{\log_e 2}{t_{\frac{1}{2}}}\tau}\, h(\tau)\, d\tau \qquad (1)$$

where $C_{Recharge}(t)$ and $C_Q(t)$ are ^3H concentration in recharge and stream water at time t, τ is the transit time in years, $t_{1/2}$ is the ^3H half-life, and "*e*" is the exponential function. Since the decay in ^3H concentration during recharge is insignificant in relation to the precision of the analysis (± 0.5 TU), the precipitation ^3H concentration, i.e., the input function in Figure 3, is used as $C_{Recharge}(t)$. Following Maloszewski and Zuber (1993), only TTD types that require at most two fitting parameters were evaluated. Thus, parallel exponential models (Seeger and Weiler, 2014;Hrachowitz et al., 2009) and exponential piston flow models (Georgek et al., 2017) are excluded here. The specific TTD types evaluated by the current study were Piston Flow (PF), Exponential (Exp), Gamma (Gam), Fixed path one-dimensional advection dispersion (ADE-1x), and Multiple path one-dimensional advection dispersion (ADE-nx) (Dwivedi et al., 2021).

3.1.2.1 Optimization of model parameters using the Downhill simplex method in conjunction with a performance criterion

The Downhill Simplex method (Nelder and Mead, 1965;Gupta, 2016) was used to evaluate the performance of each TTD (Dwivedi et al., 2021). The modified Kling Gupta efficiency or KGE' (Gupta et al., 2009;Kling et al., 2012) was used as the model performance criterion:

$$KGE' = \sqrt{\left(\frac{Cov_{m,o}}{\sigma_m \sigma_o} - 1\right)^2 + \left(\frac{\sigma_m/\mu_m}{\sigma_o/\mu_o} - 1\right)^2 + \left(\frac{\mu_m}{\mu_o} - 1\right)^2} \qquad (2)$$

In Equation (2), $Cov_{m,o}$ is the covariance between the modeled (subscript m) and observed (subscript o) time series, σ_m and σ_o represent one standard deviation, and μ_m and μ_o are the mean of the modeled and observed time series, respectively. A perfectly fitting model will have a KGE' value of zero and the worst fitting model will have a KGE' value of ∞. Following Godsey et al. (2010), the KGE' criterion was estimated in a log-transformed space. Both KGE' and the characteristics of the criterion response surface were utilized to search for the optimum model parameters (Dwivedi et al., 2021). The following ranges of model parameters were considered: Mean transit time: 1 to 50 years when using tritium, which serves as a groundwater age tracer at a time scale of 1 to 50 years (Suckow, 2014;Aggarwal, 2013;Gleeson et al., 2015). Shape parameter (α) for the Gamma TTD: 0.1 to 15 (Stewart et al. (2017). Average catchment scale Péclet number (Pe): 0.1 to 100 (Kirchner et al., 2001;Kirchner and Neal, 2013).

3.2 Multi-tracer based F_{yw} estimation

3.2.1 Mathematical development of the flux-weighted (F^*_{yw}) and unweighted (F_{yw}) fraction of young water

The fraction of young water (F_{yw}) can be estimated from the amplitude ratio of tracer concentrations in outflow and inflow for any tracer (Kirchner, 2016b;von Freyberg et al., 2018). Thus, if the amplitudes of the tracer concentrations in outflow and inflow for any period λ are $A_Q(\lambda)$ and $A_P(\lambda)$, respectively, then:

$$F_{yw}(\lambda) = \frac{A_Q(\lambda)}{A_P(\lambda)} \qquad (3)$$

This method is preferred when sufficient long-term tracer data are available and can be applied without *a priori* knowledge of the TTD type (Kirchner, 2016b). If the TTD type and its parameters are known, then F_{yw} can also be estimated (Kirchner, 2016b;von Freyberg et al., 2018;Stewart et al., 2017):

https://doi.org/10.5194/hess-2021-355
Preprint. Discussion started: 8 July 2021

$$F_{yw}(\lambda) = \int_0^{T_{yw}} h(\tau)d\tau \qquad (4)$$

where T_{yw} is the threshold age for the young water, defined as the upper limit in Equation (4) for which both Equations (3) and (4) provide the equivalent value of $F_{yw}(\lambda)$. Note that T_{yw} depends not only on the periods of sinusoidal cycles in tracer concentrations, but also on the TTD parameters.

In contrast to δ^{18}O-based F_{yw} calculations that are based on tracer fluxes in precipitation and streamflow, the ^{3}H-based F_{yw} in the current study is based on tracer concentrations in recharging and discharging deep groundwater. For consistency with the literature, we express tracer flux-based fraction of young water values as F^*_{yw} and tracer concentration-based fraction of young water values as F_{yw}. However, the mathematics in both cases generally remain the same, and we provide only the mathematical derivation for F_{yw} below, unless otherwise noted. It is assumed that the precipitation tracer flux can be represented by Equation (5), which denotes an input function of sinusoidal type with period λ:

$$PC(t) = A_P(\lambda)\sin\left(\frac{2\pi}{\lambda}t - \phi_P(\lambda)\right) + K_P(\lambda) \qquad (5)$$

where $A_P(\lambda)$, $\phi_P(\lambda)$, and $K_P(\lambda)$ are the amplitude, phase angle and a constant for a given period. Similarly, the stream water tracer flux can be represented by Equation (6), which denotes an output function of tracer fluxes with period λ:

$$QC(t) = A_Q(\lambda)\sin\left(\frac{2\pi}{\lambda}t - \phi_Q(\lambda)\right) + K_Q(\lambda) \qquad (6)$$

in which $A_Q(\lambda)$, $\phi_P(\lambda)$, and $K_Q(\lambda)$ are analogous to the variables of Equation (5). Note that A_Q is also used to refer to the ^{3}H tracer cycle in deep groundwater.

https://doi.org/10.5194/hess-2021-355
Preprint. Discussion started: 8 July 2021

The stream water tracer flux (or concentration in the case of ^3H) can be conceptualized as the time-convolution of the input tracer flux weighted by TTD (Equation 1 when using a conservative tracer). For a tracer subject to radioactive decay, we use Equation 1 of Stewart et al. (2017), which represents the contribution to streamflow of different flow paths in time and space, in addition to a decay factor $e^{-\kappa\tau}$ where $1/\kappa$ *is* the mean life of the isotope of interest. Thus,

$$QC(t) = \int_0^{\infty} PC(t-\tau)e^{-\kappa\tau}h(\tau)d\tau \qquad (7)$$

where PC(t) and QC(t) are the transient tracer fluxes in precipitation and stream water, respectively, and $h(\tau)$ is the transit time distribution or *TTD* (e.g., Equation 4 for the Gamma *TTD*).

Substitution of Equation (5) into Equation (7) yields:

$$QC(t) = \int_0^{\infty} (A_P(\lambda)\sin(\omega(t-\tau) - \phi_P(\lambda)) + K_P(\lambda))e^{-\kappa\tau}h(\tau)d\tau \qquad (8)$$

If $h(\tau)$ is a Gamma TTD, Kirchner (2016b) has shown that the amplitude damping for the outflow relative to inflow tracer signals can be estimated from the Fourier transform of *h(τ)*. For example, for a Gamma TTD with shape parameter α and scale parameter β (=mTT/ α), its power spectrum can be expressed as the following (Bain, 1982):

$$(H(\omega))^2 = \frac{1}{(1+(\omega\beta)^2)^{\alpha}} \qquad (9)$$

Thus, the amplitude damping for any period can be expressed as:

$$\frac{A_Q}{A_P}(\omega) = \frac{1}{(1+(\omega\beta)^2)^{\frac{\alpha}{2}}} \qquad (10)$$

https://doi.org/10.5194/hess-2021-355
Preprint. Discussion started: 8 July 2021

Hydrology and Earth System Sciences Discussions
Open Access

The decay factor $\exp(-\kappa\tau)$ is not considered in Equation 10. If the decay factor is considered, then the scale parameter in the Gamma TTD can be transformed to yield an expression akin to the standard Gamma TTD equation with a power spectrum equation similar to Equation 10. The subsequent expression for $A_Q/A_P\ (\omega)$ is:

$$\frac{A_Q}{A_P}(\omega) = F_{yw}(\omega) = \frac{1}{(1+\kappa\beta)^{\alpha}(1+\left(\frac{\omega\beta}{1+\kappa\beta}\right)^2)^{\frac{\alpha}{2}}} \qquad (11)$$

For a conservative tracer (e.g., $\delta^{18}O$), $\kappa=0$ in Equation 11, yielding Equation 10. Consequently, the amplitude ratio of output to input tracer fluxes can be obtained analytically for any period if the TTD parameters are already known using Expression 11. To relate the amplitude ratio to TTD through the parameter T_{yw} (Equation 4), T_{yw} can be estimated by:

$$T_{yw}(\lambda) = gaminv(\frac{A_Q}{A_P}(\lambda), \alpha, \beta) \qquad (12)$$

where $gaminv$ is the standard MATLAB® inverse Gamma function. In section S1, Equation 11 is used to compare the output:input amplitude ratios for various periods with respect to the Exponential TTD, which is a special case of the Gamma TTD. In section S2, the formulation of T_{yw} (Equation 12) is compared with the alternative recommendations of Kirchner (2016b) and Stewart et al. (2017). For $\delta^{18}O$, the applicable tracer period ranged from 2 days (due to the median daily sampling interval; see Section 2.2.2) to 5 years (the length of the high-density data record, WY 2008 to WY 2012), whereas the applicable ^3H tracer period ranged from 1 year (due to half-yearly sampling of ^3H in Tucson precipitation) to 27 years (the length of the data record).

https://doi.org/10.5194/hess-2021-355
Preprint. Discussion started: 8 July 2021

3.2.2 Estimation of F_{yw} and T_{yw} using various tracers

3.2.2.1 Estimation of F^{*}_{yw} and T^{*}_{yw} using stable water isotope tracers

Multiple methods were utilized to compare F^{*}_{yw} and T^{*}_{yw} estimates from long-term stable water isotope data during the same period. In all cases, estimates of F^{*}_{yw} were obtained using tracer flux data, i.e., as a product of tracer concentration and hydrologic flux. Daily precipitation and streamflow were used to calculate the fraction of precipitation contributing to streamflow where daily precipitation was aggregated to time steps corresponding to the availability of stable water isotope data in precipitation. The iteratively re-weighted least square (IRLS) method was used to estimate F^{*}_{yw} by fitting sinusoidal functions with periods ranging from 2 days to 5 years to tracer flux data (Kirchner, 2016b;von Freyberg et al., 2018). Additional estimates of F^{*}_{yw} were obtained using the weighted wavelet transform (WWT) method (Kirchner and Neal (2013) and the TTD method (Equation 11), also with periods of 2 days to 5 years. With respect to $\delta^{18}O$, method- and period-based F^{*}_{yw} estimates were coupled to previously established TTD parameters (Dwivedi et al., 2021), and multi-year average values of F^{*}_{yw} were used to compare between different methods (Stockinger et al. (2019); Gallart et al. (2020a). The T^{*}_{yw} was estimated as a function of period using F^{*}_{yw} estimates obtained from application of each of the three methods.

The temporal variability of $\delta^{18}O$ in precipitation was addressed by means of uncertainty analyses of F^{*}_{yw} and T^{*}_{yw}. For F^{*}_{yw}, the temporal variability of $\delta^{18}O$ was expressed as three statistics: daily mean, mean + 1 standard deviation (σ), and mean - 1σ calculated for both precipitation (P) and stream water (Q); consideration of all pair combinations resulted in total nine scenarios. For each period, the minimum, mean (referred to as the ensemble mean below), maximum, and 1σ of the F^{*}_{yw} results were computed for all nine scenarios. The T^*_{yw} process was similar but included additional uncertainty associated with the Gamma TTD parameter such that there were 27 total scenarios for each period.

3.2.2.2 Estimation of F_{yw} and T_{yw} using ^{3}H

The ^{3}H tracer data in precipitation and deep groundwater at MGC are sparse relative to δ^{18}O, especially for deep groundwater (Figure 3). As a result, application of the IRLS method to deep groundwater ^{3}H was unsatisfactory i.e., fitting a sinusoidal function to the data resulted in significant amplitude uncertainty at a period of one year. Therefore, the ^{3}H F_{yw} and T_{yw} estimates are based on the TTD method (Equations 16 and 17). Because the estimated ^{3}H-based TTD parameters demonstrated significant variability (Section 4.1.1), F_{yw} and T_{yw} uncertainty analyses followed the TTD-based F^*_{yw} and T^*_{yw} calculations derived from δ^{18}O (Section 3.2.2.1).

3.3 Estimation of discharge sensitivity of F_{yw} from δ^{18}O data

When there is a linear relationship between F_{yw} and discharge (this linear relationship has been observed at MGC up to a threshold discharge; points in Figure 7A), von Freyberg et al. (2018) suggested that the discharge sensitivity of F_{yw} for λ=1 year can be estimated by approximating the amplitude of the tracer cycle in stream water as a function of discharge alone, i.e., $A_Q=n+m*Q$, where n and m are constants. It is important to note here that what has been termed "discharge sensitivity" of F_{yw} in previous studies is in fact the response of discharge to F_{yw}. Nonetheless, if tracer cycle in precipitation has amplitude A_P, then F_{yw} can be expressed as:

$$F_{yw} = \frac{A_Q}{A_P} = \frac{n}{A_P} + \left(\frac{m}{A_P}\right) Q \qquad (13)$$

https://doi.org/10.5194/hess-2021-355
Preprint. Discussion started: 8 July 2021

Hydrology and Earth System Sciences
Open Access
Discussions

Using the expression for tracer cycle amplitude (Equation 13) and an equation similar to Equation (6) above for the sinusoidal tracer concentration cycle, the unweighted tracer cycle in stream water can be expressed as:

$$C_Q(t) = (n + mQ)\sin\left(\frac{2\pi}{\lambda}t - \phi_Q\right) + K_Q \qquad (14)$$

By fitting $C_Q(t)$ from Equation (14) to the observed tracer time series (e.g., blue points in Figure 2B), the discharge sensitivity of F_{yw}, which is equal to m/A_P and has units of 1/units of discharge, can be estimated for the annual tracer cycle. Note that von Freyberg et al. (2018) did not consider the phase angle, ϕ_Q, to be a function of discharge, because changes in ϕ_Q between high and low flows would have only a minor influence on the discharge sensitivity of F_{yw}.

Gallart et al. (2020b) noted limitations of the von Freyberg et al. (2018) approach, especially under high discharge conditions. They proposed an alternative method for discharge sensitivity estimation that is robust under high flow conditions. In the Gallart et al. (2020b) approach, F_{yw} is expressed as an exponential-type equation:

$$F_{yw} = 1 - (1 - F_o)e^{-SQ} \qquad (15)$$

where F_o (dimensionless) is the virtual F_{yw}, i.e., F_{yw} for Q=0, and S is the discharge sensitivity of F_{yw} in units of 1/units of discharge. While the approach of von Freyberg et al. (2018) assumes that A_Q is a linear function of Q, A_Q in the Gallart et al. (2020b) approach assumes a more complex function of Q. Nonetheless, using Equation (15), the tracer concentration in stream water can be expressed as:

$$C_Q(t) = A_P(1 - (1 - F_o)e^{-SQ})\sin\left(\frac{2\pi}{\lambda}t - \phi_Q\right) + K_Q \qquad (16)$$

https://doi.org/10.5194/hess-2021-355
Preprint. Discussion started: 8 July 2021

By fitting Equation 16 to the observed tracer cycle in stream water for λ = 1 year, F_o and S can be estimated. In contrast to Equation 14, the solution of Equation (16) for F_o and S is not straightforward because they appear in a single term of Equation 16. To estimate the two parameters, Gallart et al. (2020b) used a non-linear technique that may lead to parameter estimates unrelated to reality, for instance negative values of F_o.

Instead of a non-linear technique, the current study presents a practical, simplified approach. If S*Q<<1, then exp(-SQ) can be approximated by the first two terms in its Maclaurin series expansion, so that Equation 16 becomes:

$$C_Q(t) = A_P F_o \sin\left(\frac{2\pi}{\lambda}t - \phi_Q\right) + A_P(1 - F_o)SQ \sin\left(\frac{2\pi}{\lambda}t - \phi_Q\right) + K_Q \qquad (17)$$

Thus, the IRLS method can be used for estimating F_{yw} discharge sensitivity and its associated uncertainty. If S*Q <<1, Gallart et al. (2020b) have shown that the discharge sensitivity of F_{yw} should be similar to that estimated from the approach of von Freyberg et al. (2018). In the current work, we have used both the Gallart et al. (2020b) and von Freyberg et al. (2018) methods for estimating the discharge sensitivity of F_{yw}, in order to better understand the nature of transient flow paths that are activated as catchment storage changes.

https://doi.org/10.5194/hess-2021-355
Preprint. Discussion started: 8 July 2021

4 Results

4.1 ^{3}H-based TTD type, parameters, and modeled outflow tracer concentrations

4.1.1 ^{3}H-based TTD type and mTT at Marshall Gulch

Both Piston Flow (PF) and Gamma (Gam) TTDs performed adequately and yielded TTD parameters within the permissible parameter space (Table 1). However, model performance expressed in terms of KGE' was slightly better for the PF relative to the Gam TTD type (PF KGE' was 29% lower). Comparison of the PF and Gam TTDs further suggested "approximate equifinality" (Kirchner, 2016a) in the PF TTD results (Figure 4E vs. 4B). For example, three separate PF TTD model runs yielded mTTs of 32.5, 29.5, and 35.5 years (Figure 4E; Case 5 in Table S3) with very similar KGE' values (~0.4; Case 5 in Table S3). In contrast, three separate Gam TTD runs yielded similar mTTs (mTT ~ 26 years) and α parameters (5.23). Overall, the PF TTD mTT varied between 4 and 33 years with a coefficient of variation of 0.57 (Table 1), and the Gam TTD mTT and α parameters varied between 26 and 30 years (mean mTT = 27 yrs; coefficient of variation = 0.05) and 2.17 to 14.58 (unitless) (mean α = 6.53; coefficient of variation = 0.64), respectively.

4.1.2 Modeled tracer concentrations in deeper groundwater

Modeled ^{3}H concentrations in deep groundwater were generally within their observed ranges and remained within 1σ of their simulated means for both PF and Gam TTDs, but modeled ^{3}H concentration variability was lower for the Gam TTD type (Figure 5). The error bars in Figure 5 were determined by considering the analytical uncertainty in ^{3}H concentrations and are based on the first set of model runs.

Although the ADE-1x TTD-based model produced ^{3}H concentrations that were within their observed ranges, the estimated TTD parameters were sometimes at the edge of the allowable parameter space; simulated ^{3}H concentrations resultant from the ADE-nx TTD-based model were far from observed concentrations and suggest that this TTD type is not applicable at MGC.

4.2 F^*_{yw} and T^*_{yw} based on δ^{18}O

4.2.1 Comparison of δ^{18}O tracer-based F^*_{yw} estimates using various methods

Considering F^*_{yw} variability due to δ^{18}O variability in precipitation and stream water, the IRLS method yielded more variable results than the WWT or TTD-based methods, particularly for periods less than one year (Figure 6A). Note that both the IRLS and WWT methods are based on sinusoidal curve fitting to the observed tracer data, but the F^*_{yw} estimates resultant from the WWT method are less scattered because it involves spectral smoothing of data noise (Dwivedi et al., 2020;Kirchner and Neal, 2013). For a period of 1 year, F^*_{yw} estimated from the TTD-based method was higher than the corresponding estimates obtained from the IRLS and WWT methods (Figure 6A). Comparison of ensemble means (due to significant variability in F^*_{yw} estimates) for λ = 1 year indicated a F^*_{yw} ensemble mean ± 1σ of 34.9 ± 0.5% using the TTD-based method, compared to 11.4 ± 0.7% and 7.9 ± 0.2% for the IRLS and WWT methods, respectively.

4.2.2 Comparison of δ^{18}O-based T^*_{yw} estimates

As with F^*_{yw}, the T^*_{yw} results showed significantly greater variability when estimated using the IRLS method compared to the WWT or TTD-based methods, especially for periods below 0.5 years (Figure

https://doi.org/10.5194/hess-2021-355
Preprint. Discussion started: 8 July 2021

Hydrology and Earth System Sciences Discussions
Open Access

385 6B). Estimation of T^*_{yw} with any method requires *a priori* knowledge of the TTD parameters (Equation 12) that are identical to those used to calculate F^*_{yw}. For λ = 1, the ensemble T^*_{yw} means ± 1σ were 0.125 ± 0.0058 yrs (TTD), 0.008 ± 0.0013 yrs (IRLS), and 0.004 ± 0.0003yrs (WWT).

4.3 F_{yw} and T_{yw} based on ^{3}H

4.3.1 F_{yw}

390 The time series' of ^{3}H in groundwater and streamflow (Fig. 3, inset) were too sparse and coarse for reliable estimation of A_Q/A_P using the IRLS or WWT methods (Equation 3). Instead, we used the TTD method to calculate F_{yw} with model parameters drawn from section 4.1.1. The F_{yw} was characterized by a gradual increase in dF_{yw} /dλ (Figure 6C). For λ = 1, the ensemble mean-based F_{yw} was (1.6 ± 2.40) x 10^{-3} % (blue triangle in Figure 6C).

395 #### 4.3.2 T_{yw}

Although T_{yw} estimated using the TTD method gradually increased with period, dT_{yw}/d*λ* gradually declined (Figure 6D). As with the F_{yw} estimates, large error bars reflect variability in the TTD parameters. For an annual cycle, the ensemble mean-based T_{yw} was 2.03 ± 2.22 yr (blue triangle in Figure 6D).

4.4 Discharge sensitivity of annual F_{yw} estimated from δ^{18}O data

400 The discharge sensitivity of F_{yw} is the slope of F_{yw} vs. discharge, Q (Figure 7A). Following the methods of von Freyberg et al. (2018) and Gallart et al. (2020b) and for λ = 1 year, calculated discharge sensitivities were 0.09 ± 0.02 day/mm and 0.11 ± 0.02 day/mm at Marshall Gulch, respectively. However, discharge sensitivity depended on whether tracer data were weighted by streamflow. Discharge sensitivities were

0.09 ± 0.02 (mean ± standard error) and 0.11 ± 0.02 without weighting but decreased to 0.03 ± 0.01 day/mm and 0.04 ± 0.01 day/mm when the tracer data were weighted by streamflow. These estimates were computed by fitting a sinusoidal cycle of an annual period to the observed stream water $\delta^{18}O$ data. Analysis of F_{yw} vs. Q suggests that F_{yw} initially decreases with increasing Q (Figure 7A). This pattern may be due to an evaporative increase in stream water $\delta^{18}O$ under low-flow conditions, leading to an increase in A_Q, and thus an increased A_Q/A_P ratio as Q decreases (Jasechko (2019); Stockinger et al. (2017). At higher flows (Q > ~ 3.2mm/day), F_{yw} remained constant, but there is lower confidence in these estimates because the high-Q brackets of data contain fewer observations with significant variability. Given that the high flow observations correspond to periods immediately following high intensity precipitation, the results suggest an asymptotic nature of discharge sensitivity at higher flows.

5 Discussion

5.1 ^3H-based TTD type and mTT estimates

Previous estimates of TTD type and mTT at Marshall Gulch (MGC) were based on single stable isotope tracers (Heidbüchel et al., 2012;Dwivedi et al., 2021). The current work compliments these studies by using a tracer (^3H) that is applicable over decades rather than years. For both ^3H and $\delta^{18}O$ tracers, a Gamma TTD type was appropriate for MGC with mTT ~0.82 yrs (α = 0.42, unitless) using $\delta^{18}O$ and ~27 yrs (α = 6.53, unitless) using ^3H. These composite results are consistent with Stewart et al. (2010) that also noted differences in mTTs using a combination of ^3H and $\delta^{18}O$. The ^3H-based mTT estimate was close to the 26-year interval over which the amount-weighted ^3H data were available and was consistent with ages of bedrock-hosted groundwater from Dwivedi et al. (2019b). We therefore conclude that the

https://doi.org/10.5194/hess-2021-355
Preprint. Discussion started: 8 July 2021

large difference between mTT calculated from ^{3}H versus δ^{18}O can be attributed to the range of applicability of each tracer. Stable water isotopes are generally considered applicable to determine groundwater ages up to 5 years (DeWalle et al., 1997;Dwivedi et al., 2021) and are therefore appropriate for subsurface storages with faster flow (Stewart et al., 2010). In contrast, ^{3}H is generally considered applicable up to a period of 50 years (Suckow, 2014;Aggarwal, 2013) and is thus appropriate for estimating "hidden" or deep groundwater contributions to streamflow (Stewart et al., 2012). The current study that uses both tracers can separate the contributions of both quick and slow groundwater flow to streamflow in a headwater mountain catchment.

5.2 Subsurface storages

The δ^{18}O tracer is ostensibly applicable to soil water storage at MGC because the residence time of soil water is expected to be low due to high hydraulic conductivity (Heidbüchel et al., 2013;Heidbüchel et al., 2012;van der Velde et al., 2014). As a result, the δ^{18}O tracer-based TTD calculated by the current study is likely associated with soil water storage. The current work also suggests that short-term storage estimates depend on the method used to estimate F^*_{yw} and T^*_{yw}. If the short-term storage in a catchment is defined as the upper limit of water storage with age $\leq T^*_{yw}$ (or $\leq T_{yw}$), and calculated as F^*_{yw}xT^*_{yw}*Q (Jasechko et al., 2016), estimates for short-term storage at MGC vary between 0.08 mm (WWT method), 0.22 mm (IRLS method), and 10.7 (TTD method). Using a method akin to IRLS, previous reported global short-term storages ranged between 1 and 55 mm (median 14 mm) (Jasechko et al. (2016). For catchments comparable in size to MGC and for which mean annual discharge data are reported, the range narrows to between 6 mm (Rietholzbach site) and 30 mm (McDonalds B site) (Jasechko et al. (2016). Thus, the short-term storage estimates determined using various methods at MGC generally fall within the global range, albeit at the lower end for sites with subhumid climate, this may reflect the thin soils at MGC. No similar attempts were made to estimate long-term storage from ^{3}H data because of the shortcomings of the dataset.

In the traditional approach (see Rodriguez et al. (2021) and references therein), storage is a function of the tracer-based mTT multiplied by the long-term mean discharge. Application of this approach to MGC results in storage estimate of 6.7 m using an ^{3}H-based mTT of 27 years and the observed long-term streamflow (WY 2008 to WY 2017). In contrast, an equivalent modern groundwater depth of 3 m on the land surface was determined by Gleeson et al. (2015). Acknowledging such issues, Kirchner (2016a) - using stable water isotopes and virtual experiments - suggested the use of volume-weighted rather than time-weighted mTTs. However, Peters et al. (2013) and Dwivedi et al. (2021) have shown that volume-weighted mTTs and time-weighted mTTs differ by only a factor of ~2 as opposed to orders of magnitude. Volume weighted mTTs are also difficult to obtain via ^{3}H data due to the lack of multi-decade observations of both streamflow and tracer concentrations in outflow. Further, the use of mean long-term discharge is problematic as the contribution of deep groundwater to streamflow is likely to be lower than contributions from soil water or other near surface storages. Using end-member mixing analysis, Dwivedi et al. (2019b) reported a deep groundwater contribution to streamflow of 4.5% of the long-term streamflow at MGC. If this fraction is included in the storage calculation, then the storage estimate decreases to a more plausible 0.3 m. Taken together, the results of the current work suggest that the tracer-based mTT can be used to estimate storage volumes, provided they are interpreted with appropriate caution.

https://doi.org/10.5194/hess-2021-355
Preprint. Discussion started: 8 July 2021

5.3 Comparison to previous estimates of T_{yw} and F_{yw}

Previous work has proposed F_{yw} as a metric that can be used to compare hydrologic characteristics among catchments (Jasechko, 2016; Kirchner, 2016b; von Freyberg et al., 2018). Here, F_{yw} and T_{yw} estimates for MGC are compared to other study sites; in all cases, the estimates correspond to λ = 1 year.

5.3.1 Estimates from stable water isotopes

The TTD-based T^*_{yw} (0.125 ± 0.0058 yrs) was within the range reported by Kirchner (2016b) i.e., between 0.11 and 0.25 years for α ranging between 0.2 and 2, but T^*_{yw} and F^*_{yw} estimates from the IRLS and WWT methods were lower than the corresponding TTD-based metrics (Section 4.2). Gallart et al. (2020a) reported that F^*_{yw} estimates for λ = 1 year increased with higher sampling resolution (this finding was also corroborated by Stockinger et al. (2016) with F^*_{yw} values of 10.3%, 22.6%, and 30.4% resultant from weekly, high-resolution (30-minute as well as flow-dependent sampling), and "virtual thorough" sampling that involved using 5-minute discharge along with the F_{yw} vs. Q relationship to estimate F_{yw} (Table S6). The results of the current work support Gallart et al. (2020a) insofar as the TTD-based F^*_{yw} represents a thorough sampling of flowpaths with transit time between 0 and T^*_{yw} years. In this way, the TTD based F^*_{yw} results may be more reliable than estimates derived from the IRLS or WWT methods that potentially lack thorough sampling of flowpaths between the transit times of 0 and T^*_{yw} years. However, the literature on F^*_{yw} is mostly based on IRLS or similar methods with few studies reporting TTD-based results (Table 2).

In comparing the results for MGC with those of other studies (Table 2), a problem arises because most previous studies used only the IRLS method or similar method to estimate F_{yw}. At MGC, the IRLS

https://doi.org/10.5194/hess-2021-355
Preprint. Discussion started: 8 July 2021

method appears to underestimate F_{yw} relative to the TTD method as explained above. It is probably not useful to compare the TTD results from MGC with IRLS results from elsewhere; therefore, we begin by comparing the IRLS result at MGC with those from other studies.

Comparison of the IRLS-based F_{yw}^* estimates at MGC to the literature (Table 2) suggests that streamflow generation processes, hydroclimate, bedrock geology, sampling frequency of stream water, and the estimation method used all influence values of F_{yw} in ways that have not been previously reported. For example, von Freyberg et al. (2018) characterized a site with F_{yw}^* = 49% that was characterized by fast shallow groundwater flow paths during both small and large precipitation events, but another site with F_{yw}^* = 20% where dynamic flow paths changed with precipitation events of different sizes. While the discharge sensitivity of MGC (section 4.4) also suggests dynamic flow paths, these flow paths principally appear to co-evolve with changes in catchment storage. At a site with a Mediterranean sub-humid climate, Gallart et al. (2020a) reported an F_{yw}^* value of 22.6, and a meta-analysis of catchments comparable in area to MGC and located mostly in humid climates determined that F_{yw}^* (estimated as 26% greater than reported F_{yw}; von Freyberg et al. (2018)) ranged between 6 and 33% (Jasechko et al. (2016) Table S6; Table 2); however, the fractured bedrock at MGC is functionally distinct than the "watertight" bedrock characterized by Gallart et al. (2020a) and the majority of humid sites in Jasechko et al. (2016) that are comparable in size to MGC. Similarly, F_{yw}^* values reported by Clow et al. (2018), Zhang et al. (2018), and Bansah and Ali (2019) can be attributed to differences in the climate and/or bedrock characteristics between MGC and their field sites. F_{yw}^* discrepancies between MGC and mountain sites in Lutz et al. (2018) and a headwater catchment in Stockinger et al. (2019) are likely due to their relatively coarser stream water sampling frequency relative to MGC (Table 2).

Comparison of the F_{yw}^{*} at MGC to TTD-based F_{yw} estimates in the literature shows that MGC is at lower end of the range reported by Wilusz et al. (2017) for humid Plynlimon catchments in the U.K. (Table 2). We attribute these differences to methodological inconsistencies including the use of different T_{yw}^{*} values. Specifically, Wilusz et al. (2017) conducted rainfall-runoff modeling in conjunction with rank StorAge Selection (rSAS) function-based transit time modeling (more details in Harman, 2015), in order to estimate F_{yw}^{*} when T_{yw}^{*}=0.25 years, as opposed to T_{yw}^{*}=0.12 years at MGC. In other cases, differences between TTD-based F_{yw}^{*} estimates in the current study and those reported in the literature are the result of using a single period for TTD parameter estimation (e.g., Song et al. (2017); Stockinger et al. (2017)), as opposed to various periods and wavelet analysis to determine the appropriate TTD type and its parameters at MGC (Dwivedi et al., 2021). A TTD-based F_{yw}^{*} estimate (1.5%) for an oceanic, forested catchment was significantly lower than MGC and was likely due to gently sloping topography at that site versus the steep topography at MGC (Rodriguez et al. (2021) Table 2). Remondi et al. (2019) applied integrated hydrological flow and transport models to determine F_{yw}^{*} at MGC using a synthetic topography, but the results spanned almost the entire range of permissible F_{yw} values and the model performed poorly during the winter season that is the dominant recharge period (Dwivedi et al., 2021).

5.3.2 Estimates from ^{3}H

The ensemble mean F_{yw} based on annual ^{3}H cycles at MGC was 1.6 x 10^{-3} %, or effectively 0% (Figure 6C). For comparison, the lowest F_{yw} value in Stewart et al. (2017) is ~8% for a system composed of two homogeneous sub-systems, each having an mTT of 25 years with the Gamma TTD shape parameter α = 10 (unitless). We attribute this difference to either: (i) the constant T_{yw} value that Stewart et al. (2017)

https://doi.org/10.5194/hess-2021-355
Preprint. Discussion started: 8 July 2021

used for both α and tracer cycle period; or (ii) differences in the hydrogeologic settings between MGC and the Stewart et al. (2017) New Zealand catchments, or (iii) the use of multiple lumped parameter models by Stewart et al. (2017), as opposed to the F_{yw} values in the current work that are based on fitting a single *TTD* to the whole ^{3}H dataset for deep groundwater. If Equation (11) is applied to the MGC data using a Gamma TTD with parameters α = 10 (unitless) and mTT = 25 years (e.g., from Stewart et al., 2017), the resulting value of F_{yw} would be 1.1x10^{-10} %, still effectively 0%, indicating that parameter choice is not responsible for the difference. Using TTD parameter estimates from rSAS (rank StorAge Selection) functions, Rodriguez et al. (2021) reported a F_{yw} estimate of 1.8% for a forested headwater catchment that is closer to the near-zero F_{yw} estimate at MGC but may also be subject to differences in sampling protocols and/or calculation methods i.e., Rodriguez et al. (2021) sampled stream water under varying flow conditions, in contrast to baseflow sampling in this work, and used a T_{yw} value of 0.2 years.

A negligible F_{yw} at MGC calls into question of the suitability of the ^{3}H-based F_{yw} approach for deeper groundwater. The fractured bedrock storage at MGC has a large mTT (~27 years), and the annual tracer cycle will be highly damped as a result ($F_{yw} \sim 0$; section 4.3.1). From the standpoint of the IRLS method (Equation 3), the ^{3}H data in precipitation or deep groundwater, if useful, should have an amplitude A_P or A_Q greater than the ^{3}H measurement precision (0.5 TU, Section 2.2.3) for some period between 1 and 27 years. At MGC, this is true for A_P at periods greater than 19 years, but not for A_Q at any period up to 27 years (Section S3); consequently, the available data are inadequate for calculating F_{yw}. This is apparent in the lack of consistent annual periodicity in the Tucson Basin precipitation data (Figure 3), which may not be possible to overcome even with a much larger ^{3}H dataset.

https://doi.org/10.5194/hess-2021-355
Preprint. Discussion started: 8 July 2021

Hydrology and Earth System Sciences Discussions

5.4 Dynamic catchment behavior revealed by the discharge sensitivity

The discharge sensitivity of F_{yw} at MGC suggests that flowpaths in shallow storages restructure and reorganize dynamically as catchment storage changes (Figure 7B). Using the discharge sensitivity of F_{yw} for various Swiss catchments, von Freyberg et al. (2018) suggested three cases (Figure 7B) for dynamic evolution of flowpaths: Case 1: catchments with high F_{yw} but low discharge sensitivity in which fast flowpaths dominate and persist during both large and small events; Case 2: catchments with low F_{yw} but high discharge sensitivity in which different flowpaths dominate during large and small events; and Case 3: catchments with low F_{yw} and low discharge sensitivity in which slow flowpaths dominate and persist during both large and small events. When evaluated without any flow-weighting, the discharge sensitivity of F_{yw} at MGC suggests that it falls under Case 2 i.e., reorganization of flowpaths with change in catchment storage, as recently noted in the more humid Plynlimon, U.K. catchments (Wilusz et al., 2017). The linear-regression approach to calculating F_{yw} specifically indicates a threshold of ~ 3.2 mm/day above which the mean F_{yw} does not increase with Q at MGC (Figure 7A). Using a method similar to Jasechko et al. (2016) with estimates for F_{yw} and T_{yw} based on Gamma TTD parameters from Dwivedi et al. (2021) using their "Method 1" and Equation (17) in this work, discharge of 3.2 mm/day results in a short-term storage estimate of 0.05 m. Thus, after a threshold of 0.05 m short-term near-surface storage at MGC, the current study supports that infiltration may activate deeper groundwater flowpaths (Dwivedi et al. (2019b).

There is evidence for a global inverse relationship between topographic slope and F_{yw} (Jasechko et al., 2016; 2017). Topographic roughness and fractured bedrock permeability may also play roles in promoting infiltration to fractured-bedrock aquifers in steep mountainous catchments once shallow

https://doi.org/10.5194/hess-2021-355
Preprint. Discussion started: 8 July 2021

storage is exceeded. A case in point is the difference between recharge seasonality in two mountain blocks of similar lithology: the Santa Catalina Mountains, Arizona where MGC is located (mainly winter recharge) and the neighboring Rincon Mountains, Arizona (both summer and winter recharge). Eastoe and Wright (2019) attributed the difference in infiltration of summer rainwater to topographic control by the orientation of pegmatite sheets that are steeply dipping in the Santa Catalina Mountains versus sub-horizontal in the Rincon Mountains that is more conducive to infiltration during high intensity summer precipitation events. This current work suggests the presence of an additional factor, threshold storage, that contributes to observed inverse relationships between F_{yw} and topographic slope.

5.5 Limitations of the proposed approach

Considered together, F_{yw} and its discharge sensitivity provide complimentary information about transient flowpaths (Figure 8A). Increasing catchment storage specifically results in reorganization of transient flow paths and activation of deep flow paths rather than simple acceleration of flow along any given path. Importantly, the magnitude of the F_{yw} metric depends on the method used to estimate it. Recent literature has suggested limitations of the δ^{18}O-based F_{yw} metric (e.g., Jacobs et al. (2018) Stockinger et al. (2017) Jasechko et al. (2016). However, the literature has mainly reported F_{yw} estimates based on either IRLS or similar sinusoidal curve fitting methods for annual or seasonal tracer cycles (Table 2; Table S6). The current work contributes to the growing body of F_{yw} research by quantifying the variability of IRLS-based results at a mountain headwater catchment (Figure 6A). For an annual tracer cycle, F_{yw} from the IRLS method was one-third of F_{yw} from the TTD method, and it is therefore likely that previously reported F_{yw} estimates may be underestimated. This would have significant implications for F_{yw}-based understanding

https://doi.org/10.5194/hess-2021-355
Preprint. Discussion started: 8 July 2021

of contaminant and nutrient transport, surface water quality (Kirchner, 2016a; Jasechko et al., 2016), and estimation of TTD parameters (Lutz et al., 2018). As a result, future studies utilizing IRLS or similar methods may wish to report F_{yw} for various periods, in addition to the annual period, in order to better constrain the variability of the results. Future studies that reported TTD-based results would also be useful to characterize the methodological sensitivity of F_{yw} across a broader range of natural systems.

The use of a ^{3}H-based F_{yw} metric has been recommended toward an improved understanding of deep and/or slow flowpaths contributing to streamflow (Jacobs et al., 2018;Jasechko, 2019). However, the current study highlights that the ^{3}H-based F_{yw} metric may be inappropriate when there are insufficient deep groundwater data, which is a general limitation in groundwater aquifers including MGC (Rodriguez et al., 2021;Gleeson et al., 2015). This limitation can also lead to significant variability in the estimated Gamma TTD parameters when the ^{3}H tracer is applied to the question of "hidden streamflow" (Stewart et al., 2010;Stewart et al., 2012;Seeger and Weiler, 2014;Jacobs et al., 2018). In contrast to F_{yw}, the ^{3}H-based mTT metric does not depend on any particular period of tracer cycles in inflow and outflow, but aggregation errors may lead to estimates of mTT that are low by several orders of magnitude relative to known mTTs from virtual experiments, especially in heterogeneous catchments such as MGC (Kirchner, 2016b; Stewart et al. (2017). The current work also demonstrates that the ^{3}H-based mTT can lead to greatly over-estimated total deep groundwater storage estimates. To address this issue, appropriate long-term discharge estimates, not including storm runoff, are critical to accurate storage calculations (Section 5.2). Finally, the current results support the use of multiple ("lumped") parameter models, qualified by site-specific hydrogeological information to reduce aggregation errors in real catchments, but

https://doi.org/10.5194/hess-2021-355
Preprint. Discussion started: 8 July 2021

acknowledge that model parameters may be difficult to constrain in the multiple parameter approach (Stewart et al. (2017); Jacobs et al. (2018); Hrachowitz et al. (2009)).

6 Conclusions

This study supports concurrent application of multiple metrics for a more complete understanding of the transient flow paths and storage volumes that contribute to streamflow in a sub-humid mountain headwater catchment. Among the various combinations of tracers and metrics that were tested, the most appropriate metrics at MGC included $\delta^{18}O$-based F_{yw}, discharge sensitivity, and shallow storage mTT, in addition to ^3H-based deeper storage mTT. Application of the weighted wavelet transform (WWT), iteratively re-weighted least square (IRLS), and transit time distribution (TTD) methods to annual cycles of $\delta^{18}O$ in stream water resulted in flux-based F_{yw} values of 7.9 ± 0.2%, 11.4 ± 0.7%, and 34.9 ± 0.5%, respectively. The current study therefore constrains the degree to which F_{yw} depends on the method of estimation. At MGC, the Gamma TTD was preferred on the basis that it thoroughly sampled flow paths between a transit time of zero and a threshold age for young water. In comparison, the IRLS results were scattered over the periods of interest and were only approximately one-third of the TTD-based estimate an annual period; WWT results were similar to IRLS but showed much less scatter owing to spectral smoothing of the data.

The Gamma TTD-based mTT using ^3H data was 27 years. The same methodology yielded an MTT of 0.82 years when based on $\delta^{18}O$ (Dwivedi et al., 2021); hence, we conclude that the former mTT may correspond to groundwater stored in fractured bedrock, whereas the latter applies to shallow storages in the soil profile. The shape parameters of the ^3H-based Gamma TTD at MGC demonstrated

https://doi.org/10.5194/hess-2021-355
Preprint. Discussion started: 8 July 2021

significant variability arising from the short length and inconsistent seasonal cyclicity of the available ^3H time series data that precluded adequate estimation of F_{yw} in fractured-bedrock groundwater. Although data quality could be addressed by longer-term observation and attention to precision, variations of ^3H in precipitation at some locations may restrict the applicability of this approach. In summary, using $\delta^{18}O$-based F_{yw} together with its discharge sensitivity was an effective method with which to quantify the dynamic nature of shallow groundwater flowpaths at MGC. Beyond a threshold F_{yw} in short-term storage, additional infiltration is likely to activate deeper groundwater flow paths.

Author contributions:

R. Dwivedi: Conceptualization, Formal analysis, Investigation, Methodology, Validation, Visualization

C. Eastoe: Writing – original draft preparation, Writing – review & editing

J. F. Knowles: Writing – review & editing

J. McIntosh: Funding acquisition, Project administration, Resources, Supervision, Writing – original draft preparation, Writing – review & editing

T. Meixner: Funding acquisition, Project administration, Resources, Supervision, Writing – original draft preparation, Writing – review & editing

P. A. "Ty" Ferre: Funding acquisition, Project administration, Resources, Supervision, Writing – original draft preparation, Writing – review & editing

R. Minor: Writing – review & editing

G. Barron-Gafford: Writing – review & editing

N. Abramson: Data curation, Writing – review & editing

M. Stanley: Resources, Writing – review & editing

J. Chorover: Funding acquisition, Project administration, Resources, Supervision, Writing – original draft preparation, Writing – review & editing

Acknowledgments

We would like to thank Drs. J. Kirchner and J. von Freyberg for guiding the fraction of young water analysis, and Drs. J. Kirchner and M. Stewart for helpful comments on a preliminary version of this paper. The authors acknowledge support from National Science Foundation Grants EAR 1331408 and 0724958 to the Santa Catalina Mountains and Jemez River Basin Critical Zone Observatory. RD also acknowledges the Geological Society of America for Graduate Student Research and Horton Research Grants, and the The University of Arizona Graduate and Professional Student Council for Research and Travel grants; TM, JM, TF, and RD acknowledge additional support from the Water Resources Research Center 104(b). The corresponding author would like to thank his wife, Jessie Dwivedi, and their children, Darcy and Noah Dwivedi, for their patience and support during this project. Some aspects of this study are based on previously published data. The authors declare no conflicts of interest.

References

Aggarwal, P. K.: Introduction, in: Isotope methods for dating old groundwater, edited by: Suckow, A., Aggarwal, P. K., and Araguas-Araguas, L., International Atomic Energy Agency, Vienna, 1-4, 2013.

Ajami, H., Troch, P. A., Maddock, T., Meixner, T., and Eastoe, C.: Quantifying mountain block recharge by means of catchment-scale storage-discharge relationships, Water Resources Research, 47, 1-14, 10.1029/2010wr009598, 2011.

Bain, L.: Gamma distribution, in: Encyclopedia of statistical Sciences, edited by: Kotz, S., and Johnson, N. L., 292-298, 1982.

Bansah, S., and Ali, G.: Streamwater ages in nested, seasonally cold Canadian watersheds, Hydrological Processes, 33, 495-511, 10.1002/hyp.13373, 2019.

Clow, D. W., Mast, M. A., and Sickman, J. O.: Linking transit times to catchment sensitivity to atmospheric deposition of acidity and nitrogen in mountains of the western United States, Hydrological Processes, 32, 2456-2470, 10.1002/hyp.13183, 2018.

https://doi.org/10.5194/hess-2021-355
Preprint. Discussion started: 8 July 2021

Hydrology and Earth System Sciences
Open Access
EGU
Discussions

Creed, I. F., and Noordwijk, M. v.: Chapter 1- Forests, Trees and Water on a Changing Planet: A Contemporary Scientific Perspective, in: Forest and Water on a Changing Planet: Vulnerability, Adaptation and Governance Opportunities: A Global Assessment Report, edited by: Creed, I. F., and Noordwijk, M. v., Vienna, 13-24, 2018.

DeWalle, D. R., Edwards, P. J., Swistock, B. R., Aravena, R., and Drimmie, R. J.: Seasonal isotope hydrology of three Appalachian forest catchments, Hydrol. Process., 11, 1895-1906, 1997.

Dickinson, W. R., Hirschberg, D. M., Pitts, G., Stephen, G., and Bolm, S. K.: Spatial digital database of the geologic map of Catalina Core Complex and San Pedro Trough, Pima, Pinal, Gila, Graham, and Cochise Counties, Arizona, U.S. Geological Survey, Menlo Park, CA, 1-25, 2002.

Doney, S. C., Glover, D. M., and Jenkins, W. J.: A model function of the global bomb tritium distribution in precipitation, 1960–1986, Journal of Geophysical Research, 97, 5481, 10.1029/92jc00015, 1992.

Dwivedi, R., Eastoe, C., Knowles, J. F., Hamann, L., Meixner, T., Ferre, P. A. T., Castro, C., Wright, W. E., Niu, G.-Y., Minor, R., Barron-Gafford, G. A., Abramson, N., Mitra, B., Papuga, S. A., Stanley, M., and Chorover, J.: An improved practical approach for estimating catchment-scale response functions through wavelet analysis, Hydrological Processes, 35, 1-20, https://doi.org/10.1002/hyp.14082, 2021.

Eastoe, C., and Towne, D.: Regional zonation of groundwater recharge mechanisms in alluvial basins of Arizona: Interpretation of isotope mapping, Journal of Geochemical Exploration, 194, 134-145, 10.1016/j.gexplo.2018.07.013, 2018.

Eastoe, C. J., Gu, A., and Long, A.: The Origins, Ages and Flow Paths of Groundwater in Tucson Basin: Results of a Study of Multiple Isotope Systems, in: Groundwater Recharge in a Desert Environment: The Southwestern United States, edited by: Hogan, J. F., Phillips, F. M., and Scanlon, B. R., American Geophysical Union, Washington, D. C., 2004.

Eastoe, C. J., and Wright, W. E.: Hydrology of Mountain Blocks in Arizona and New Mexico as Revealed by Isotopes in Groundwater and Precipitation, Geosciences, 9, 461, 10.3390/geosciences9110461, 2019.

Frisbee, M. D., Wilson, J. L., Gomez-Velez, J. D., Phillips, F. M., and Campbell, A. R.: Are we missing the tail (and the tale) of residence time distributions in watersheds?, Geophysical Research Letters, 4633–4637, 10.1002/grl.50895, 2013.

Gallart, F., Valiente, M., Llorens, P., Cayuela, C., Sprenger, M., and Latron, J.: Investigating young water fractions in a small Mediterranean mountain catchment: Both precipitation forcing and sampling frequency matter, Hydrological Processes, 34, 3618-3634, 10.1002/hyp.13806, 2020a.

Gallart, F., von Freyberg, J., Valiente, M., Kirchner, J. W., Llorens, P., and Latron, J.: Technical note: An improved discharge sensitivity metric for young water fractions, Hydrology and Earth System Sciences, 24, 1101-1107, 10.5194/hess-24-1101-2020, 2020b.

Georgek, J. L., Kip Solomon, D., Heilweil, V. M., and Miller, M. P.: Using tracer-derived groundwater transit times to assess storage within a high-elevation watershed of the upper Colorado River Basin, USA, Hydrogeology Journal, 26, 467-480, 10.1007/s10040-017-1655-4, 2017.

Godsey, S. E., Aas, W., Clair, T. A., de Wit, H. A., Fernandez, I. J., Kahl, J. S., Malcolm, I. A., Neal, C., Neal, M., Nelson, S. J., Norton, S. A., Palucis, M. C., Skjelkvåle, B. L., Soulsby, C., Tetzlaff, D., and Kirchner, J. W.: Generality of fractal 1/f scaling in catchment tracer time series, and its implications for catchment travel time distributions, Hydrological Processes, 24, 1660-1671, 10.1002/hyp.7677, 2010.

Gupta, H. V., Kling, H., Yilmaz, K. K., and Martinez, G. F.: Decomposition of the mean squared error and NSE performance criteria: Implications for improving hydrological modelling, Journal of Hydrology, 377, 80-91, 10.1016/j.jhydrol.2009.08.003, 2009.

Harpold, A., Brooks, P., Rajagopal, S., Heidbuchel, I., Jardine, A., and Stielstra, C.: Changes in snowpack accumulation and ablation in the intermountain west, Water Resources Research, 48, 1-11, 10.1029/2012wr011949, 2012.

Heidbüchel, I., Troch, P. A., Lyon, S. W., and Weiler, M.: The master transit time distribution of variable flow systems, Water Resources Research, 48, 1-19, 10.1029/2011wr011293, 2012.

Heidbüchel, I., Troch, P. A., and Lyon, S. W.: Separating physical and meteorological controls of variable transit times in zero-order catchments, Water Resources Research, 49, 7644-7657, 10.1002/2012wr013149, 2013.

Holleran, M. E.: Quantifying catchment scale soil variability in Marshall Gulch, Santa Catalina Mountains Critical Zone Observatory, M.S. thesis, Department of Soil, Water and Environmental Science, The University of Arizona, Tucson, AZ, 102 pp., 2013a.

Holleran, M. E.: Quantifying catchment scale soil variability in Marshall Gulch, Santa Catalina Mountains Critical Zone Observatory, M.S. , Department of Soil, Water and Environmental Science, The University of Arizona, Tucson, 102 pp., 2013b.

Jacobs, S. R., Timbe, E., Weeser, B., Rufino, M. C., Butterbach-Bahl, K., and Breuer, L.: Assessment of hydrological pathways in East African montane catchments under different land use, Hydrology and Earth System Sciences, 22, 4981-5000, 10.5194/hess-22-4981-2018, 2018.

Jasechko, S., Kirchner, J. W., Welker, J. M., and McDonnell, J. J.: Substantial proportion of global streamflow less than three months old, Nature Geoscience, 9, 126-129, 10.1038/ngeo2636, 2016.

Jasechko, S., Wassenaar, L. I., and Mayer, B.: Isotopic evidence for widespread cold-season-biased groundwater recharge and young streamflow across central Canada, Hydrological Processes, 31, 2196-2209, 10.1002/hyp.11175, 2017.

Jasechko, S.: Global Isotope Hydrogeology―Review, Reviews of Geophysics, 57, 835-965, 10.1029/2018rg000627, 2019.

Kirchner, J. W., Feng, X., and Neal, C.: Catchment-scale advection and dispersion as a mechanism for fractal scaling in stream tracer concentrations, Journal of Hydrology, 254, 82-101, 2001.

https://doi.org/10.5194/hess-2021-355
Preprint. Discussion started: 8 July 2021

Kirchner, J. W., and Neal, C.: Universal fractal scaling in stream chemistry and its implications for solute transport and water quality trend detection, Proceedings of the National Academy of Sciences of the United States of America, 110, 12213-12218, 10.1073/pnas.1304328110, 2013.
Kirchner, J. W.: Aggregation in environmental systems -Part 2: Catchment mean transit times and young water fractions under hydrologic nonstationarity, Hydrology and Earth System Sciences, 20, 299-328, 10.5194/hess-20-299-2016, 2016a.
Kirchner, J. W.: Aggregation in environmental systems- Part 1: Seasonal tracer cycles quantify young water fractions, but not mean transit times, in spatially heterogeneous catchments, Hydrology and Earth System Sciences, 20, 279-297, 10.5194/hess-20-279-2016, 2016b.
Kling, H., Fuchs, M., and Paulin, M.: Runoff conditions in the upper Danube basin under an ensemble of climate change scenarios, Journal of Hydrology, 424-425, 264-277, 10.1016/j.jhydrol.2012.01.011, 2012.
Kohler, T., and Marselli, D.: Mountains and Climate Change - From Understanding to Action, 75 p., 2009.
Lutz, S. R., Krieg, R., Müller, C., Zink, M., Knöller, K., Samaniego, L., and Merz, R.: Spatial Patterns of Water Age: Using Young Water Fractions to Improve the Characterization of Transit Times in Contrasting Catchments, Water Resources Research, 54, 4767-4784, 10.1029/2017wr022216, 2018.
Lyon, S. W., Desilets, S. L. E., and Troch, P. A.: A tale of two isotopes: differences in hydrograph separation for a runoff event when using δD versus δ18O, Hydrological Processes, 23, 2095-2101, 10.1002/hyp.7326, 2009.
Maloszewski, P., and Zuber, A.: Principles and practice of calibration and validation of mathematical models for the interpretation of environmental tracer data in aquifers, Advances in Water Resources, 16, 173-190, 1993.
McDonnell, J. J.: Beyond the water balance, Nature Geoscience, 10, 396-396, 10.1038/ngeo2964, 2017.
McDonnell, J. J., Evaristo, J., Bladon, K. D., Buttle, J., Creed, I. F., Dymond, S. F., Grant, G., Iroume, A., Jackson, C. R., Jones, J. A., Maness, T., McGuire, K. J., Scott, D. F., Segura, C., Sidle, R. C., and Tague, C.: Water sustainability and watershed storage, Nature Sustainability, 1, 378-379, 10.1038/s41893-018-0099-8, 2018.
Nelder, J. A., and Mead, R.: A simplex method for function minimization, The Computer Journal, 7, 308-313, 1965.
Pelletier, J. D., and Rasmussen, C.: Geomorphically based predictive mapping of soil thickness in upland watersheds, Water Resources Research, 45, 1-15, 10.1029/2008wr007319, 2009.
Peters, N. E., Burns, D. A., and Aulenbach, B. T.: Evaluation of High-Frequency Mean Streamwater Transit-Time Estimates Using Groundwater Age and Dissolved Silica Concentrations in a Small Forested Watershed, Aquatic Geochemistry, 20, 183-202, 10.1007/s10498-013-9207-6, 2013.
PRISM Gridded Climate Data for the Location: Lat: 32.4263 Lon: -110.7610 Elev: 7703ft: http://prism.oregonstate.edu access: June 6, 2018, 2018.
Remondi, F., Botter, M., Burlando, P., and Fatichi, S.: Variability of transit time distributions with climate and topography: A modelling approach, Journal of Hydrology, 569, 37-50, 10.1016/j.jhydrol.2018.11.011, 2019.
Rodriguez, N. B., and Klaus, J.: Catchment Travel Times From Composite StorAge Selection Functions Representing the Superposition of Streamflow Generation Processes, Water Resources Research, 55, 9292-9314, 10.1029/2019wr024973, 2019.
Rodriguez, N. B., Pfister, L., Zehe, E., and Klaus, J.: Testing the truncation of travel times with StorAge Selection functions using deuterium and tritium as tracers, Hydrol. Earth Syst. Sci., 25, 401–428, 10.5194/hess-2019-501, 2021.
Seeger, S., and Weiler, M.: Reevaluation of transit time distributions, mean transit times and their relation to catchment topography, Hydrology and Earth System Sciences, 18, 4751-4771, 10.5194/hess-18-4751-2014, 2014.
Song, C., Wang, G., Liu, G., Mao, T., Sun, X., and Chen, X.: Stable isotope variations of precipitation and streamflow reveal the young water fraction of a permafrost watershed, Hydrological Processes, 31, 935-947, 10.1002/hyp.11077, 2017.
Stewart, M. K., Morgenstern, U., and McDonnell, J. J.: Truncation of stream residence time: how the use of stable isotopes has skewed our concept of streamwater age and origin, Hydrological Processes, 24, 1646-1659, 10.1002/hyp.7576, 2010.
Stewart, M. K., Morgenstern, U., McDonnell, J. J., and Pfister, L.: The 'hidden streamflow' challenge in catchment hydrology: a call to action for stream water transit time analysis, Hydrological Processes, 26, 2061-2066, 10.1002/hyp.9262, 2012.
Stewart, M. K., Morgenstern, U., Gusyev, M. A., and Maloszewski, P.: Aggregation effects on tritium-based mean transit times and young water fractions in spatially heterogeneous catchments and groundwater systems, and implications for past and future applications of tritium, Hydrology and Earth System Sciences, 21, 4615–4627, 10.5194/hess-21-4615-2017, 2017.
Stockinger, M. P., Bogena, H. R., Lücke, A., Diekkrüger, B., Cornelissen, T., and Vereecken, H.: Tracer sampling frequency influences estimates of young water fraction and streamwater transit time distribution, Journal of Hydrology, 541, 952-964, 10.1016/j.jhydrol.2016.08.007, 2016.
Stockinger, M. P., Lücke, A., Vereecken, H., and Bogena, H. R.: Accounting for seasonal isotopic patterns of forest canopy intercepted precipitation in streamflow modeling, Journal of Hydrology, 555, 31-40, 10.1016/j.jhydrol.2017.10.003, 2017.
Stockinger, M. P., Bogena, H. R., Lücke, A., Stumpp, C., and Vereecken, H.: Time variability and uncertainty in the fraction of young water in a small headwater catchment, Hydrology and Earth System Sciences, 23, 4333-4347, 10.5194/hess-23-4333-2019, 2019.
Suckow, A.: The age of groundwater – Definitions, models and why we do not need this term, Applied Geochemistry, 50, 222-230, 10.1016/j.apgeochem.2014.04.016, 2014.
USGS NED 1 arc-second n33w111 1 x 1 degree ArcGrid 2018: https://viewer.nationalmap.gov/basic/, access: May 15, 2018, 2018.

United Nations: TRANSFORMING OUR WORLD: THE 2030 AGENDA FOR SUSTAINABLE DEVELOPMENT, United Nations, 35 p., 2015.

United Nations: The United Nations World Water Development Report 2021: Valuing Water, UNESCO, Paris., 187, 2021.

van der Velde, Y., Heidbüchel, I., Lyon, S. W., Nyberg, L., Rodhe, A., Bishop, K., and Troch, P. A.: Consequences of mixing assumptions for time-variable travel time distributions, Hydrological Processes, 29, 1-15, 10.1002/hyp.10372, 2014.

Viviroli, D., Weingartner, R., and Messerli, B.: Assessing the hydrological significance of the world's mountains, Mountain Research and Development, 23, 32-40, 10.5167/uzh-110514
10.1659/02764741(2003)023[0032:ATHSOT]2.0.CO;2, 2003.

Viviroli, D., Dürr, H. H., Messerli, B., Meybeck, M., and Weingartner, R.: Mountains of the world, water towers for humanity: Typology, mapping, and global significance, Water Resources Research, 43, 1-13, 10.1029/2006wr005653, 2007.

von Freyberg, J., Allen, S. T., Seeger, S., Weiler, M., and Kirchner, J. W.: Sensitivity of young water fractions to hydro-climatic forcing and landscape properties across 22 Swiss catchments, Hydrology and Earth System Sciences, 22, 3841-3861, 10.5194/hess-22-3841-2018, 2018.

Wilusz, D. C., Harman, C. J., and Ball, W. P.: Sensitivity of Catchment Transit Times to Rainfall Variability Under Present and Future Climates, Water Resources Research, 53, 231-256, 10.1002/2017WR020894, 2017.

Zhang, Q., Knowles, J. F., Barnes, R. T., Cowie, R. M., Rock, N., and Williams, M. W.: Surface and subsurface water contributions to streamflow from a mesoscale watershed in complex mountain terrain, Hydrological Processes, 32, 954-967, 10.1002/hyp.11469, 2018.

https://doi.org/10.5194/hess-2021-355
Preprint. Discussion started: 8 July 2021

Figures and Tables:

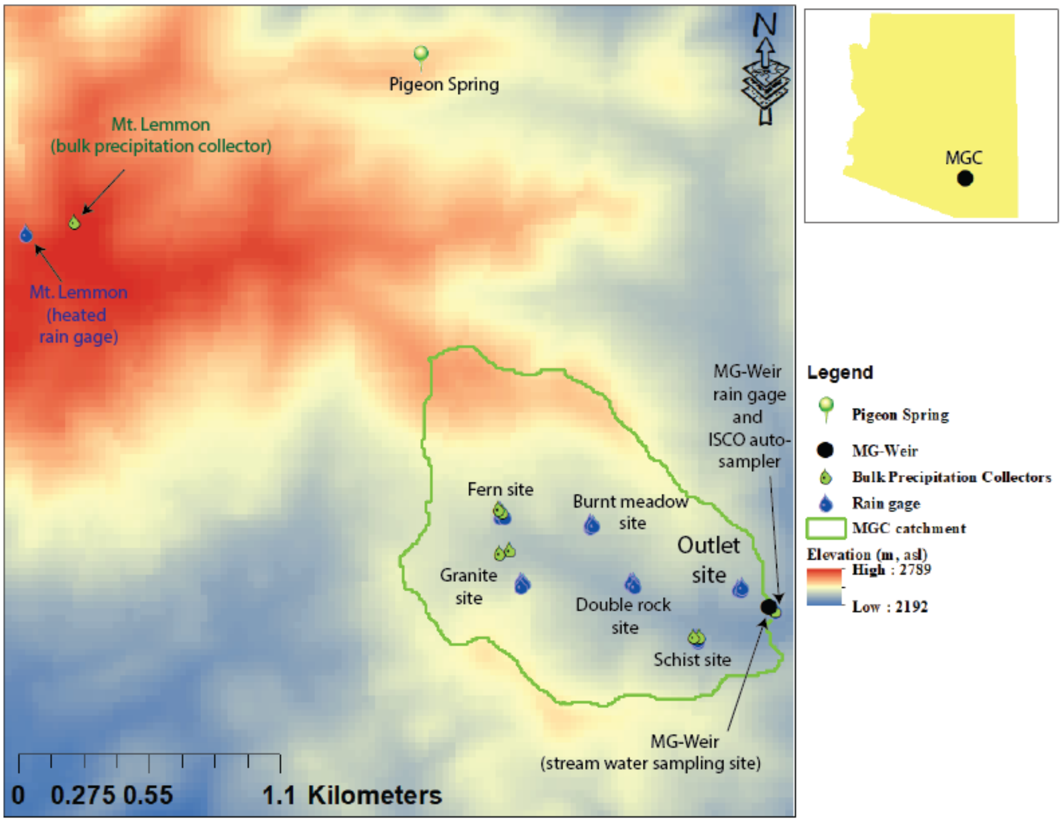

820 Figure 1: Marshall Gulch Catchment (MGC; the catchment boundary is shown in green), located within the Santa Catalina Mountains Critical Zone Observatory (SCM-CZO) in southeast Arizona, USA (inset map), along with the precipitation, stream water, and deep groundwater collection sites. The digital elevation model data are from the U.S. Geological Survey (2018).

https://doi.org/10.5194/hess-2021-355
Preprint. Discussion started: 8 July 2021

Hydrology and Earth System Sciences
Open Access
EGU
Discussions

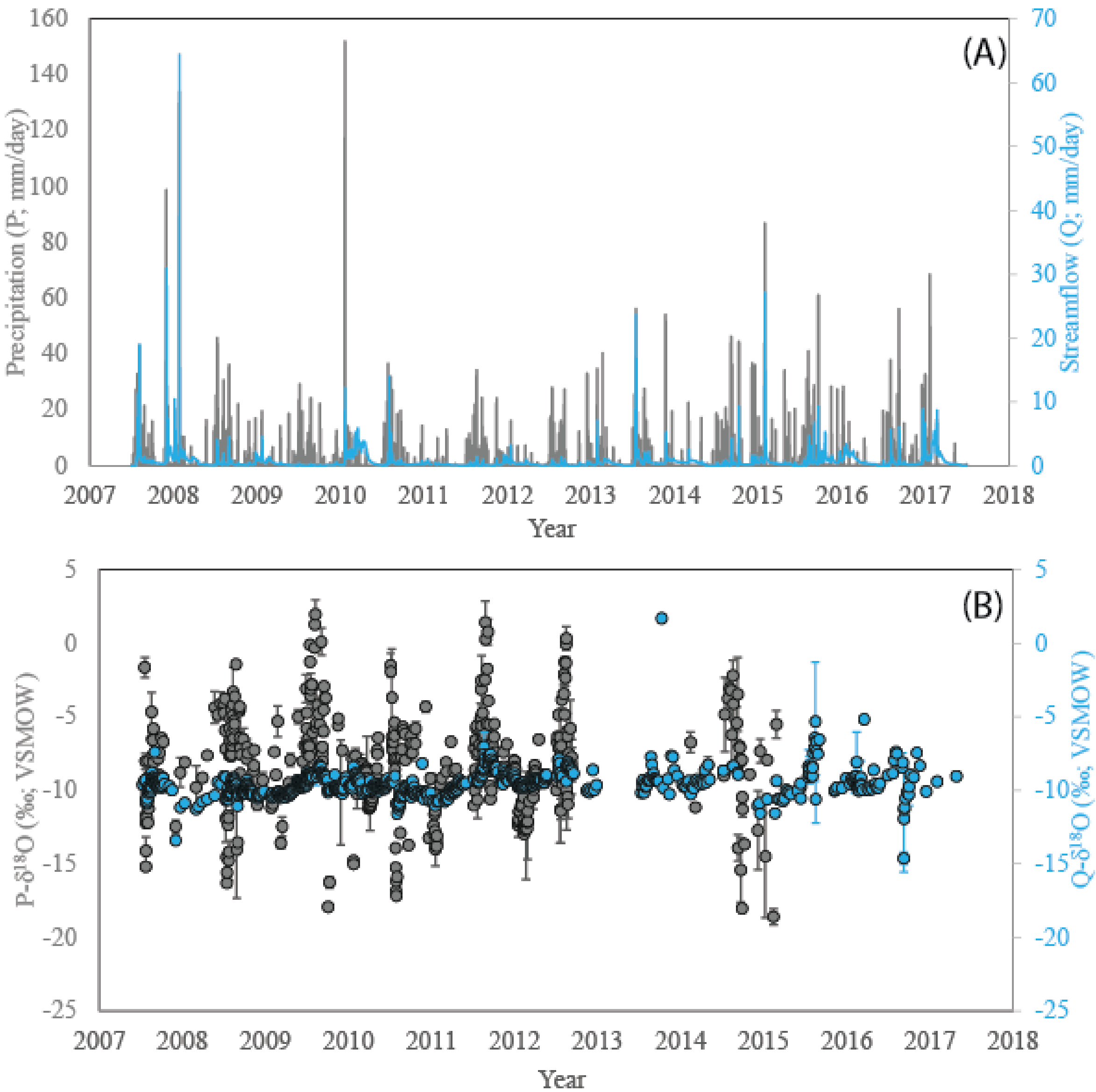

825
Figure 2. (A) Timeseries plots of daily precipitation (P) and streamflow (Q) and (B) $\delta^{18}O$ in P and Q from water year (WY) 2008 through WY 2017. The error bars in (B) show one standard deviation.

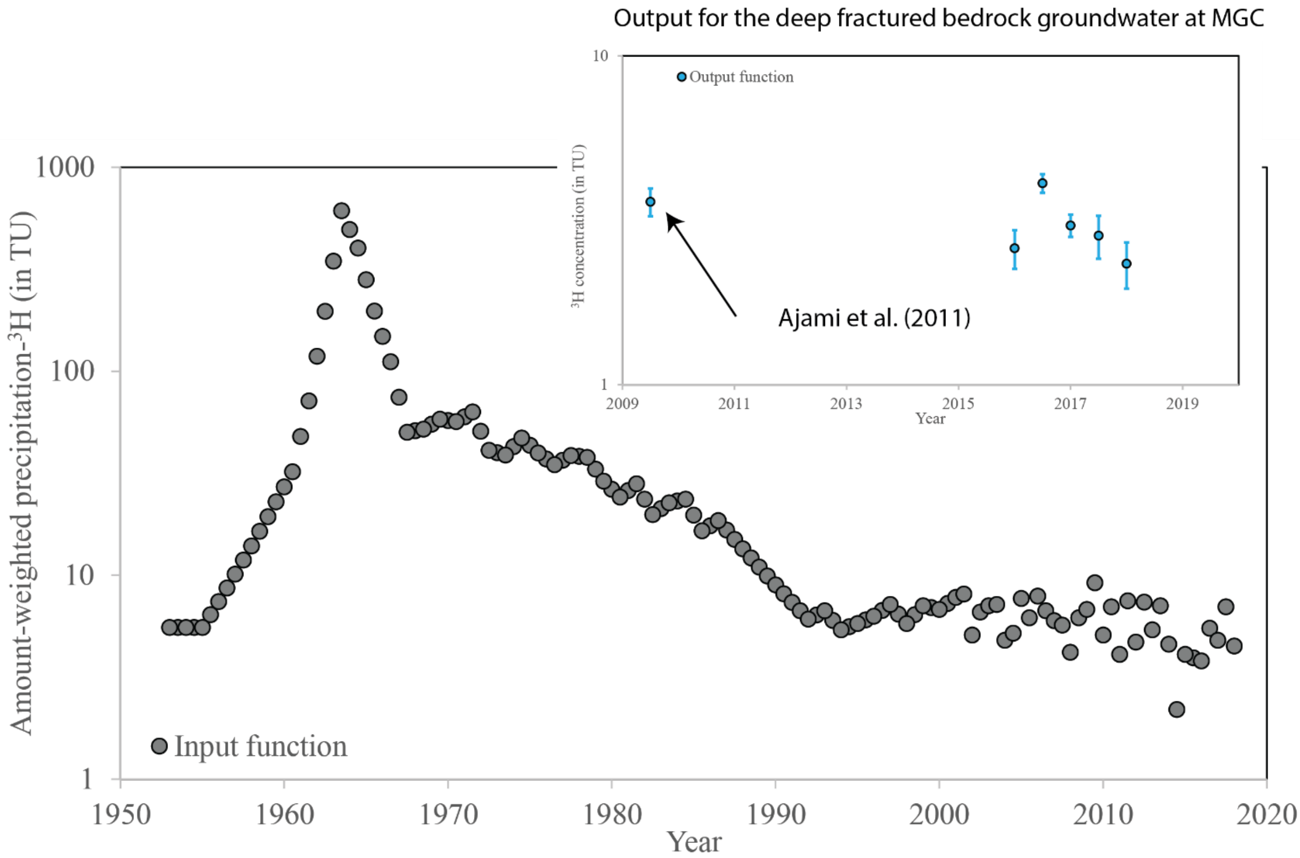

830 Figure 3. Amount-weighted ^{3}H concentration in precipitation (data from Eastoe et al. (2004); The Environmental Isotope Laboratory, The University of Arizona; Eastoe, unpublished data; Figure S1), and ^{3}H concentrations in deep fractured bedrock groundwater (blue points; a combination of MG-Weir site and Pigeon Spring; see Figure 1).

https://doi.org/10.5194/hess-2021-355
Preprint. Discussion started: 8 July 2021

Hydrology and Earth System Sciences Discussions

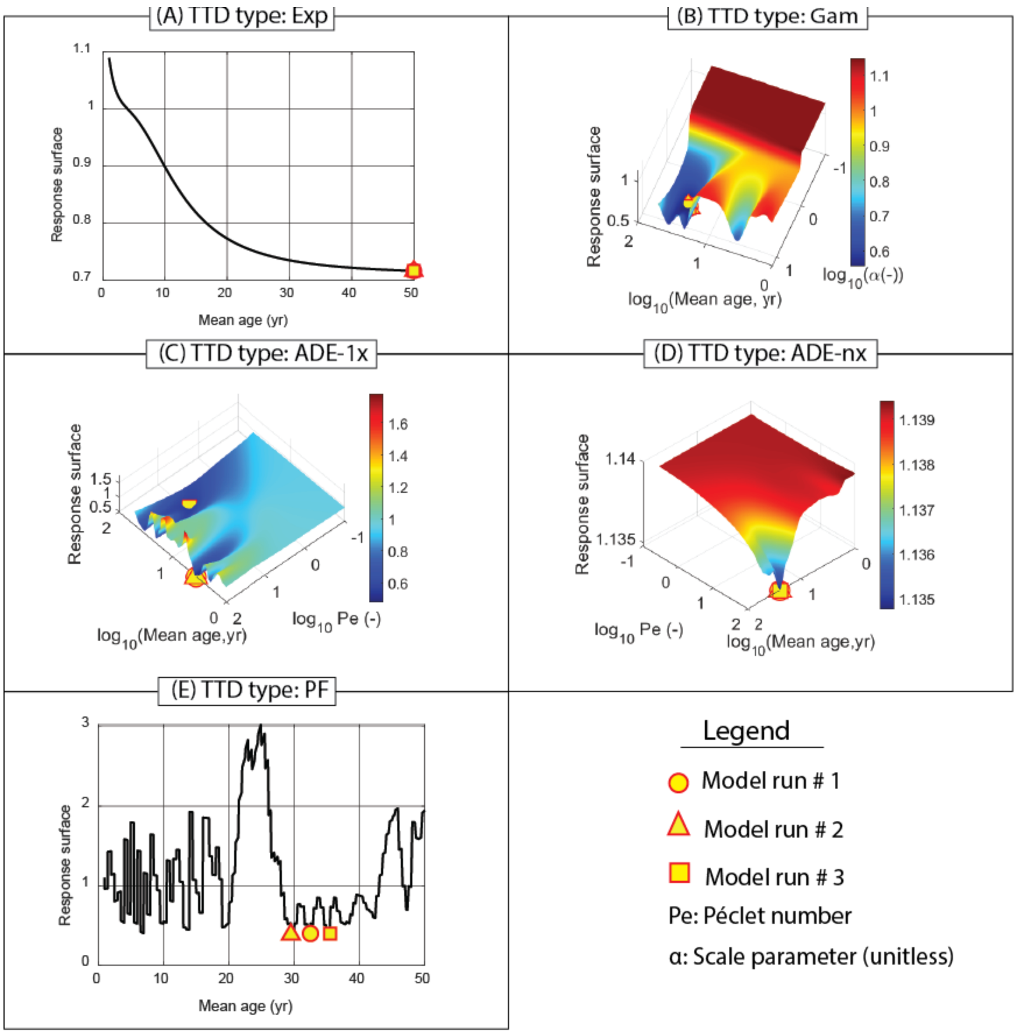

840 Figure 4. Response surfaces for various TTD types when using ^3H input and output functions as shown in Figure 3. Results for the three separate model runs are shown as different symbols.

https://doi.org/10.5194/hess-2021-355
Preprint. Discussion started: 8 July 2021

Hydrology and Earth System Sciences
Open Access
EGU
Discussions

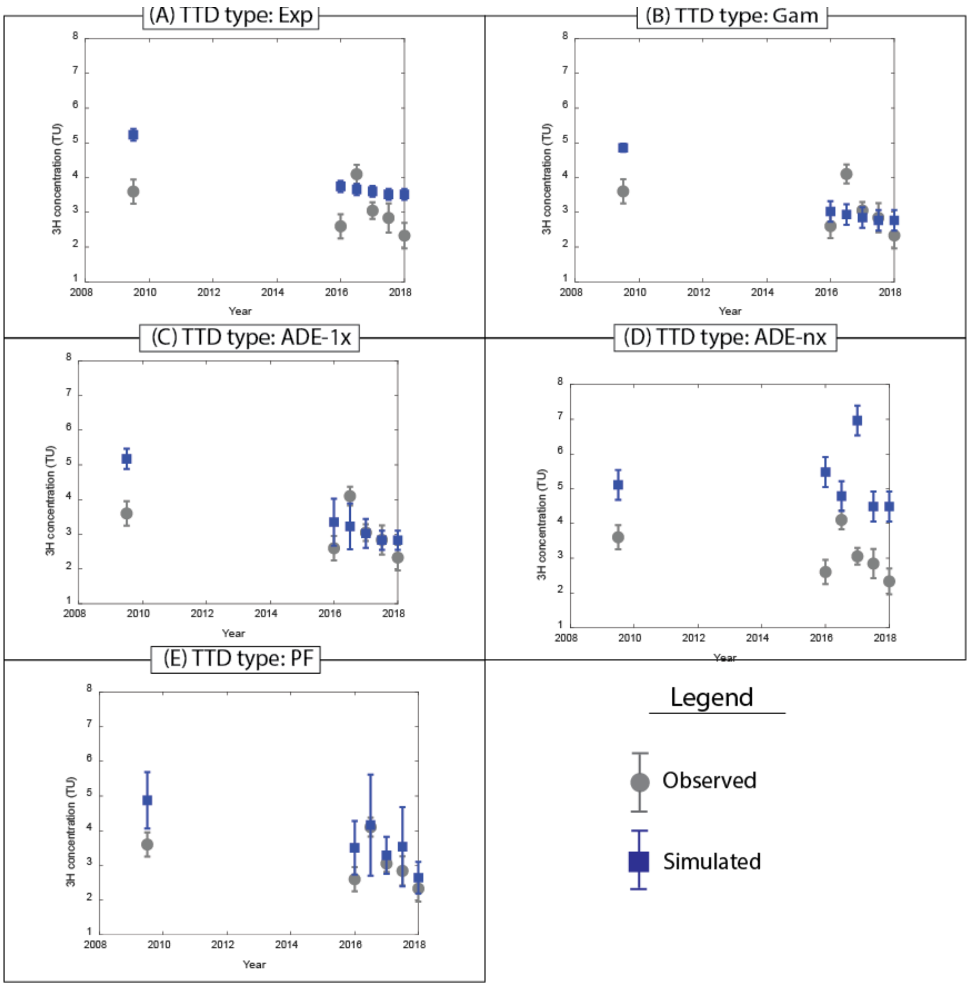

Figure 5. Observed (gray points and error bars) and modeled (blue points and error bars) ^{3}H concentration in deeper groundwater for (A) Exp, (B) Gam, (C) ADE-1x, (D) ADE-nx, and (E) PF TTD types. Error bars for the modeled concentrations represent one standard deviation of all the modeled concentrations for the first model run (i.e., run #1 in Table S3), based on uncertainty in amount-weighted ^{3}H concentrations in precipitation and deeper groundwater.

https://doi.org/10.5194/hess-2021-355
Preprint. Discussion started: 8 July 2021

Hydrology and Earth System Sciences
Open Access
Discussions

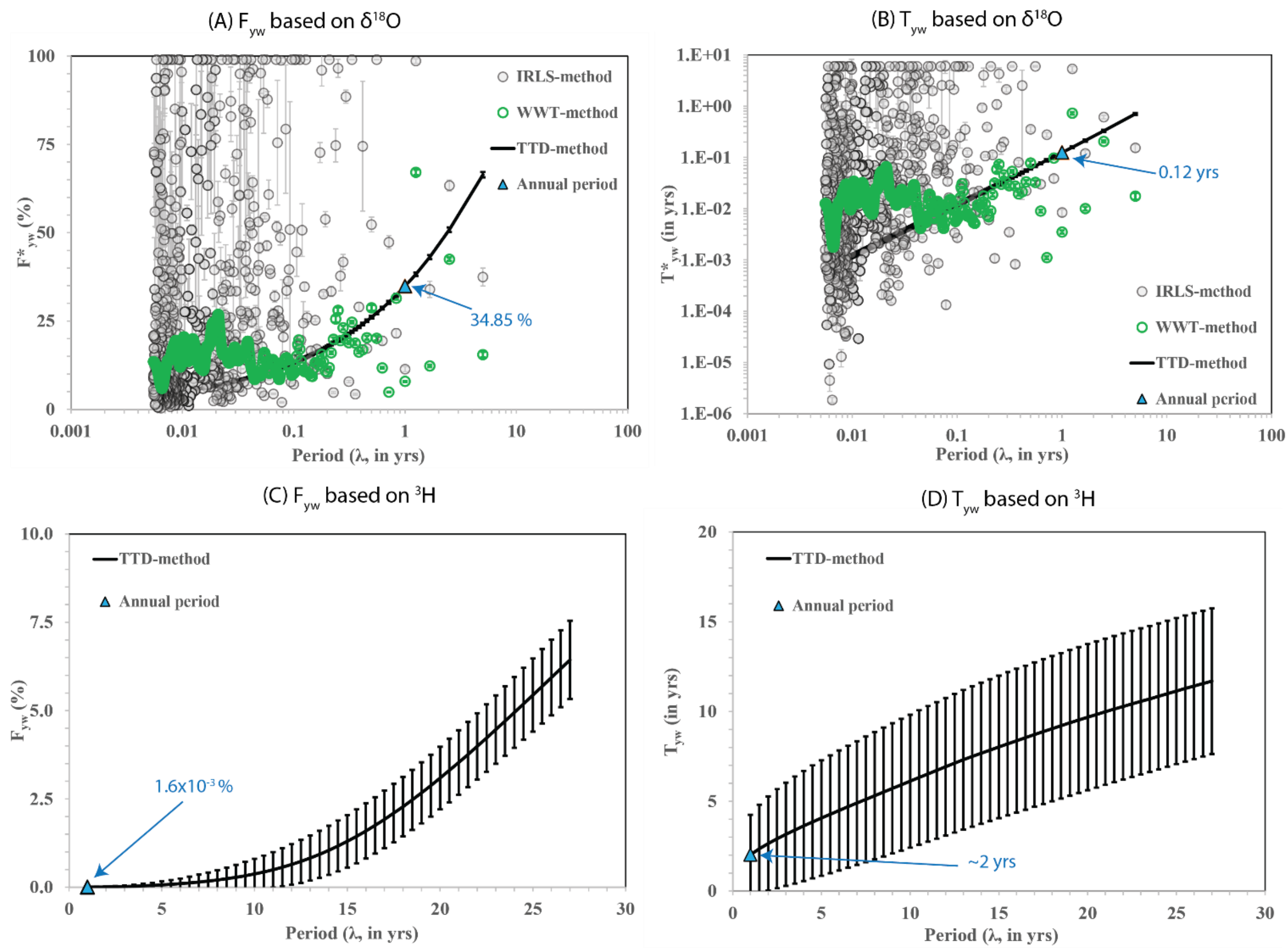

Figure 6. (A and B): F^*_{yw} (ensemble mean) and T^*_{yw} (ensemble mean) vs. period (λ), based on $\delta^{18}O$ data and (C and D): F_{yw} (ensemble mean) and T_{yw} (ensemble mean) vs. period (λ), based on ^3H data. The blue triangles in each plot show the ensemble mean of F^*_{yw} (or F_{yw}) and T^*_{yw} (or T_{yw}) values for λ = 1 year, calculated using the TTD method.

https://doi.org/10.5194/hess-2021-355
Preprint. Discussion started: 8 July 2021

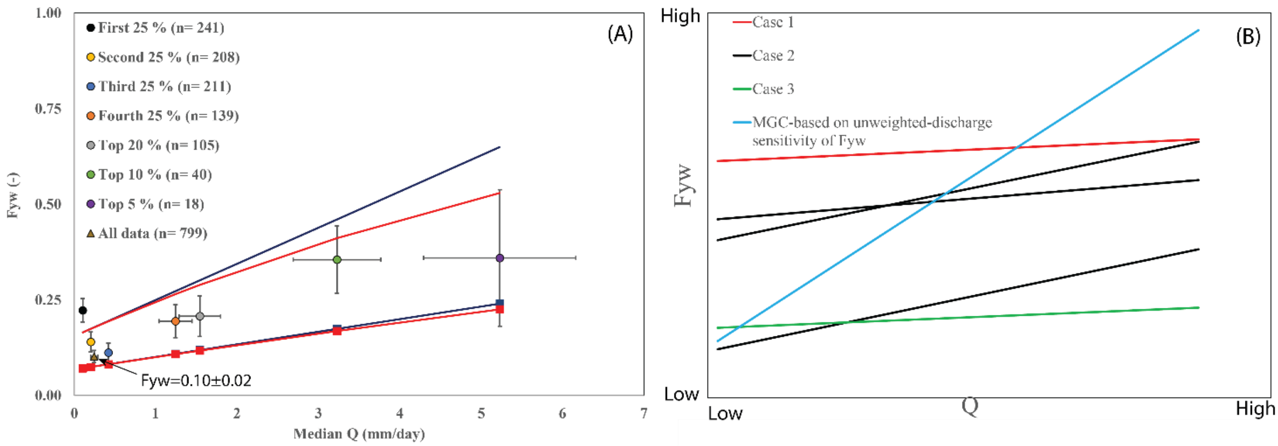

Figure 7.(A) Relationship between F_{yw} with discharge for various flow regimes (total number of observations for each flow regime shown in plot legend) computed using the methods of von Freyberg et al. (2018) and Gallart et al. (2020b) with (solid lines with square markers) and without (solid lines) flow-weighting when estimating the discharge sensitivity parameters. (B) Relationship between F_{yw} with Q with respect to the framework proposed by von Freyberg et al. (2018) (see section 5.4 for more details). Note, the blue line in (B) is the inferred F_{yw} from discharge at MGC using the discharge sensitivity of F_{yw} calculated following von Freyberg et al. (2018) without considering flow-weighting. The horizontal and vertical error bars in (A) correspond to standard errors in Q and F_{yw}, respectively.

Hydrology and Earth System Sciences
Open Access
Discussions

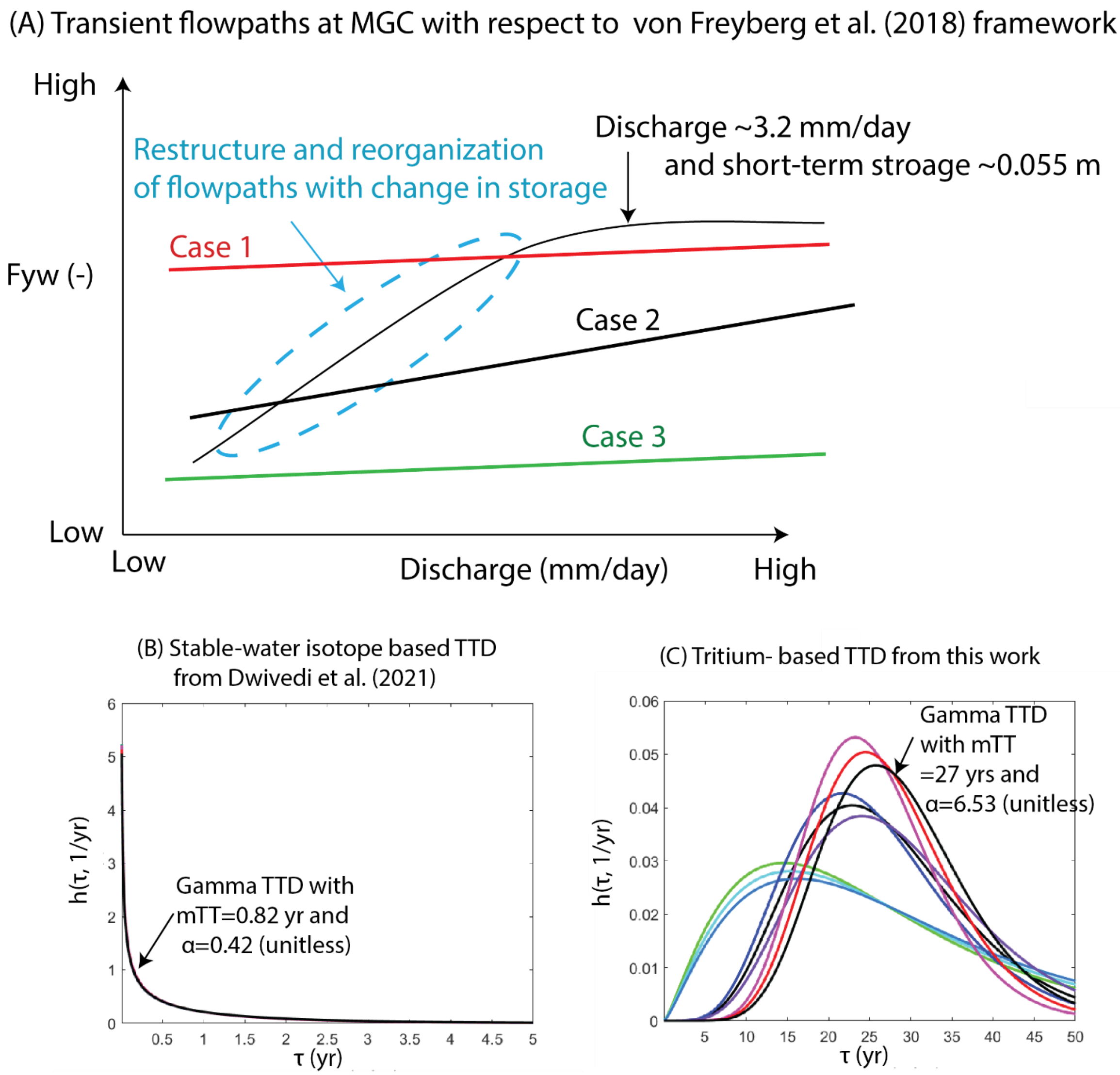

Figure 8. Novel contributions of this work in terms of inferred transient nature of flowpaths that restructure with catchment storage and threshold short-term storage after which the propensity for precipitation to infiltrate and activate deep groundwater increases. (A) transit time distribution or TTD ($h(\tau)$) and TTD parameters estimated using tritium, which compliments previous stable water isotope-based TTD estimates at the same site (Dwivedi et al., 2021). (B) The nine visually indistinguishable $h(\tau)$ curves are based on stable water isotope data and show TTDs with mean transit time (mTT) of 0.82±0.03 (mean ± one standard deviation) and α=0.42±0.001 (unitless). (C) The nine $h(\tau)$ curves are based on tritium and correspond to TTDs with mean transit time (mTT) of 27±1.4 and α=6.53±4.21 (unitless). The black curves in (B) and (C) show Gamma TTDs with TTD parameters of mTT=0.82 yr and α=0.42 (unitless) and mTT=27 yr and α=6.53 (unitless), respectively.

https://doi.org/10.5194/hess-2021-355
Preprint. Discussion started: 8 July 2021

Table 1. Estimated TTD parameters for various TTD types. The TTD parameters in columns (2) and (3) are based on the input and output functions shown in Figure 3. The TTD parameter statistics in columns (5) through (14) are based on the first set of model runs that consider amount-weighted ^{3}H concentration uncertainty in precipitation and concentration uncertainty in deep groundwater (Table S3). Parameter 1 is the mean transit time (in years). Parameter 2 is not applicable for the PF TTD type and is the scale parameter α (unitless) for the Exp and Gam TTD and the Pe parameter for the ADE-1x and ADE-nx TTD types. The parameter α is set to 1 for the Exp TTD type. KGE' is the modified Kling-Gupta Efficiency, which ranges between 0 (for the best fitting model) and infinity (for the worst fitting model).

				Parameter 1					Parameter 2				
TTD type	Parameter 1	Parameter 2	KGE'	Min	Mean	One std	CV	Max	Min	Mean	One std	CV	Max
Piston flow	32.50	0.00	0.40	4.00	21.25	12.11	0.57	33.00	NA				
Exponential	50.00	1.00	0.72	46.77	49.64	1.08	0.02	50.00	NE				
Gamma	26.34	5.23	0.56	25.92	27.04	1.36	0.05	30.40	2.17	6.53	4.21	0.64	14.58
ADE-1x	3.63	100.00	0.48	3.63	29.42	11.31	0.38	46.97	2.24	47.85	49.54	1.04	100.00
ADE-nx	24.44	100.00	1.13	23.98	24.43	0.27	0.01	24.74	100.00	100.00	0.00	0.00	100.00

NA: not applicable; NE: not estimated; Min: minimum; One std: one standard deviation; CV: coefficient of variation; and Max: maximum.

Table 2. Synthesis of F^*_{yw} estimates reported in literature including the current study. The F^*_{yw} values for studies shown in bold were obtained by scaling F_{yw} estimates by a factor of 26% from von Freyberg et al. (2018).

895

Date source	Study site	F^*_{yw} for annual tracer cycle (method used)	Mean topographic gradient (%)	Sampling frequency	Climate
This study	MGC	7.9 (WWT), 11.4 (IRLS), and 34.9 (TTD)	40	median daily data	Sub-humid
von Freyberg et al. (2018)	Erlenbach, Lumpenenbach, Reitholzbach, and Vogelbach out of 22 catchments	20 to 49 (IRLS)	14.6 to 28.9	Biweekly	Humid to temperate continental climate
Jasechko et al. (2016)	Brugga - Oberried, DE; Botorpstrommen - Gunnebo, SE; Rietholzbach - Mosnang (Pegel), CH; McDonalds B	6 to 33 (periodic regression method)	Not provided	~ monthly	Humid (Brugga – Oberried, McDonalds B); warm and temperate (Botorpstrommen - Gunnebo);

https://doi.org/10.5194/hess-2021-355
Preprint. Discussion started: 8 July 2021

Hydrology and Earth System Sciences Discussions

	Lebanon State Forest, USA				temperate humid (Rietholzbach - Mosnang Pegel);
Gallart et al. (2020a)	Can Vila, Spain	22.6 (least square fitting)	25.6	Flow-dependent 30 minutes to weekly	Mediterranean sub-humid
Song et al. (2017)	Zuomaokong watershed, Qinghai-Tibet Plateau	26 (TTD)	4.5	Daily	Permafrost watershed
Wilusz et al. (2017)	Lower Hafren and Tanllwyth, UK	30 to 55 (TTD)	Not provided	Weekly	humid sites
Zhang et al. (2018)	Boulder Creek watershed, USA	8 to 28 (convolution integral method)	Not provided	Weekly	Alpine, subalpine, and Montane
Lutz et al. (2018)	Bode catchment, Germany	1.3 to 19 (IRLS and ordinary least square)	16.5 (sites in mountains)	Monthly	Cold and wet in high elevations

https://doi.org/10.5194/hess-2021-355
Preprint. Discussion started: 8 July 2021

Hydrology and Earth System Sciences
Discussions

Bansah and Ali (2019)	South Tobacco Creek watershed, Canada	42 to 91 (sinusoidal curve fitting)	Not provided	mostly weekly, but also higher during storms	Sub-humid
Clow et al. (2018)	Andrews Creek, CO, and Andrews spring, CO, USA out of 11 catchments	19 to 21 (multiple regression method)	85 to 102	Monthly	Cold and wet during winter and warm and dry during summer
Stockinger et al. (2017)	Wusteback headwater catchment, Germany	13 to 16 (multiple linear regression) and 14 to 16 (TTD)	Not provided	Weekly	humid
Stockinger et al. (2019)	Wusteback headwater catchment, Germany	5 to ~16 (IRLS)	Not provided	Weekly	humid

https://doi.org/10.5194/hess-2021-355
Preprint. Discussion started: 8 July 2021

Rodriguez et al. (2021)	Weierbach Catchment, Luxembourg	1.5 (TTD-based method that uses StorAge Selection functions (more details in Rodriguez and Klaus (2019))	71% area with slope between 0-9% and 29 % area with slope between 9 to 96% (Rodriguez and Klaus (2019))	Sub-daily sampling for stable water isotopes and bi-weekly for tritium	Temperate and semi-oceanic